

---

# OBTAINING INTERPRETABLE PARAMETERS FROM REPARAMETERIZING LONGITUDINAL MODELS: TRANSFORMATION MATRICES BETWEEN GROWTH FACTORS IN TWO PARAMETER-SPACES

---

A PREPRINT

**Jin Liu\***

Department of Biostatistics  
Virginia Commonwealth University

**Robert A. Perera**

Department of Biostatistics  
Virginia Commonwealth University

**Le Kang**

Department of Biostatistics  
Virginia Commonwealth University

**Robert M. Kirkpatrick**

Department of Psychiatry  
Virginia Commonwealth University

**Roy T. Sabo**

Department of Biostatistics  
Virginia Commonwealth University

May 29, 2022

## ABSTRACT

The linear spline growth model (LSGM) is a popular tool for examining nonlinear change patterns, which approximates complex patterns by attaching at least two linear segments. Among such models, the linear-linear piecewise change pattern is the most straightforward. An earlier study has proved that other than the intercept and slopes, the knot (or change-point), at which two linear segments join together, can be estimated as a growth factor in a reparameterizing longitudinal model in the latent growth curve modeling framework. However, the reparameterized coefficients no longer related directly to the underlying developmental process and therefore lacked meaningful, substantive interpretation, although they were simple functions of the original parameters. This study proposes transformation matrices between parameters in the original and reparameterized frame so that the coefficients related directly to the underlying change pattern can be derived from reparameterized ones to be interpretable. Additionally, the study extends the existing linear-linear piecewise model to the framework of individual measurement occasions and investigates predictors for the individual-differences in change patterns. We present the proposed methods by simulation studies and a real-world data analysis. Our simulation studies demonstrate that the proposed model generally estimate the parameters of interest unbiasedly, precisely and exhibit appropriate confidence interval coverage. An empirical example using longitudinal mathematics scores shows that the model can estimate the growth factor coefficients and path coefficients that directly relate to the underlying developmental process and therefore provide meaningful interpretation. We also provide the corresponding code for the proposed models.

**Keywords** Linear spline growth models · Unknown knots · Individually-varying time points · Time-invariant covariates · Simulation studies

## 1 Introduction

Longitudinal studies of change are popular in various disciplines to evaluate individual growth over time. If a process under investigation is followed for a long enough time duration, it is likely to exhibit some degree of nonlinear change in which the curve has a nonconstant relationship to recorded time. One possible model to examine nonlinear

---

\*CONTACT Jin Liu. Email: Veronica.Liu0206@gmail.com

individual change pattern is a piecewise linear latent growth model (Chou et al., 2004; Harring et al., 2006; Cudeck and Harring, 2010; Kohli, 2011; Kohli et al., 2013; Kohli and Harring, 2013; Sterba, 2014), also known as the linear spline growth model (Grimm et al., 2016a). By attaching at least two linear pieces, the linear spline (or piecewise linear) functional form can approximate more complex underlying change patterns. Previous studies have demonstrated a broad application of linear spline trajectory. It has been employed to assess post-surgical rehabilitation (Riddle et al., 2015; Dumenci et al., 2019), the learning process of a specific task (Cudeck and Klebe, 2002), the onset of alcohol abuse (Li et al., 2001) and intellectual development (Marcoulides, 2018).

One major challenge of analyzing linear piecewise change patterns is to decide the location of the change-point or ‘knot’ that indicates the occurrence of the change in the developmental process. Although empirical researchers can pre-specify knot driven by domain knowledge, for example, Flora (2008); Sterba (2014); Riddle et al. (2015); Dumenci et al. (2019), in most cases, the knot is unknown. Marcoulides (2018) proposed to fit a pool of candidate models with a knot at different locations and select the ‘best’ one using the BIC criterion. By building a multiphase mixed-effects model, Cudeck and Klebe (2002) demonstrated that the change-point can also be a random coefficient that allows individuals to make the transition from one phase to another at different time points. Knots have been estimated successfully using frequentist (Cudeck and du Toit, 2003; Harring et al., 2006; Kwok et al., 2010; Kohli, 2011; Kohli et al., 2013; Kohli and Harring, 2013; Preacher and Hancock, 2015) and Bayesian (Dominicus et al., 2008; McArdle and Wang, 2008; Wang and McArdle, 2008; Muniz Terrera et al., 2011; Kohli et al., 2015a; Lock et al., 2018) mixed-effects models and growth models (including latent growth models and growth mixture models).

The most intuitive linear spline function is a bilinear spline growth model (or linear-linear piecewise model). Not only can this functional form identify a process that is theoretically two stages with different rates of change (Riddle et al., 2015; Dumenci et al., 2019), but it also can help approximate other nonlinear change patterns (Kohli et al., 2015a,b; Sullivan et al., 2017). Harring et al. (2006) developed a linear-linear piecewise model with an unknown fixed knot with a unified functional form of two linear pieces through reparameterization, which is realized by re-expressing growth factors as linear combinations of their original forms. Kohli (2011), Kohli et al. (2013) and Grimm et al. (2016a) derived the growth coefficients that directly related to the underlying change patterns from the estimated coefficients using *Mplus*. By implementing this model, Kohli et al. (2013) examined the development in each stage and estimated a fixed knot for procedural learning task research.

Preacher and Hancock (2015) extended the model with an unknown fixed knot to estimate the knot’s variance simultaneously, in which the knot is not expected to be the same and then is viewed as an additional growth factor besides the intercept and two slopes in the latent growth curve (LGC) modeling framework. More importantly, they predicted individual differences in the knot by allowing obesity status as a predictor. By re-examining a data set containing longitudinal records of plasma phosphate, they demonstrated the linear-linear functional form with an unknown random knot is useful. However, one drawback of this model lies in that it is fitted in a reparameterizing framework. The reparameterized coefficients no longer related directly to the underlying developmental process, and therefore lacked meaningful, substantive interpretation.

Accordingly, we propose (inverse-) transformation matrices to re-reparameterize the mean vector and variance-covariance matrix of growth factors in the reparameterized setting to be the coefficients that directly related to the underlying change pattern so that they are interpretable. More importantly, we extend the model proposed by Preacher and Hancock (2015) by allowing time-invariant covariates (TICs) to predict individual differences in the initial status and rate-of-change of each stage so that these covariates may account for the heterogeneity in trajectories instead of that only in the knot location. When estimating a knot with considering its variability, the reparameterization was realized by Taylor series expansion. In this study, we conduct an intensive simulation study to investigate the conditions under which this approximation does not affect the model performance meaningfully.

Additionally, we propose the model in the framework of individual measurement occasions. (Cook and Ware, 1983; Mehta and West, 2000; Finkel et al., 2003). This can occur when time is measured precisely (e.g., exact date and time of measurement), or if responses are self-initiated or randomly assigned. For instance, in an adolescent smoking study, participants were asked to complete a questionnaire on pocket computers immediately after smoking (Hedeker et al., 2006). One possible way to fit growth models with individual measurement occasions is the definition variable approach, in which the ‘definition variables’ are defined as observed variables that are employed to adjust model parameters to individual-specific values (Mehta and West, 2000; Mehta and Neale, 2005). In our case, these individual-specific values are individual measurement occasions.

The proposed method fills an existing gap by describing how to obtain interpretable parameters from the reparameterizing longitudinal model, the linear-linear piecewise latent growth model with an unknown random knot in the framework of individual-measurement occasions. It also explores predictors of between-individual differences in the change patterns. We examine the proposed method by intensive simulation studies to investigate whether the approximation introduced by the Taylor series expansion affects the model performance.

The remainder of this article is organized as follows. In the method section, we first present the model specification of the bilinear spline growth model with time-invariant covariates to estimate a knot with its variability (the full model). Next, we introduce how to reparameterize growth factors and the corresponding path coefficients from the TICs to the growth factors to make them estimable in the SEM framework and transform them back after estimation for interpretation purposes. We then propose one possible reduced model to estimate the knot without considering variability as a parsimonious backup. We then describe the model estimation as well as the Monte Carlo simulation design for model evaluation. In the result section of simulation studies, we present the evaluation of the model performance concerning the non-convergence rate, the proportion of improper solutions, as well as the estimating effects, including the relative bias, the empirical standard error (SE), the relative root-mean-squared-error (RMSE) and the empirical coverage for a nominal 95% confidence interval of each parameter of interest. In the application section, by applying the proposed model to a longitudinal data set of mathematics achievement scores from the Early Childhood Longitudinal Study, Kindergarten Class of 2010 – 11 (ECLS-K: 2011), we give a set of feasible recommendations for real-world practice. Finally, discussions are framed concerning the model’s limitations as well as future directions.

## 2 Method

### 2.1 Model Specification

In this section, we briefly describe a bilinear growth model with an unknown random knot and time-invariant covariates used to analyze nonlinear change patterns, estimate the knot with its variability, and predict individual differences in trajectories. The linear-linear piecewise latent growth model, which is an extension of LGC, specifies a separate linear function for each of the two stages of the developmental process for each individual, shown in Figure 1. In the framework of individual measurement occasions, the measure for the  $i^{th}$  individual at the  $j^{th}$  time point is

$$y_{ij} = \begin{cases} \eta_{0i} + \eta_{1i}t_{ij} & t_{ij} \leq \gamma_i \\ \eta_{0i} + \eta_{1i}\gamma_i + \eta_{2i}(t_{ij} - \gamma_i) & t_{ij} > \gamma_i \end{cases}, \quad (1)$$

where  $y_{ij}$  and  $t_{ij}$  are the measurement and measurement occasion of the  $i^{th}$  individual at time  $j$ . In Equation (1),  $\eta_{0i}$ ,  $\eta_{1i}$ ,  $\eta_{2i}$  and  $\gamma_i$  are individual-level intercept, first slope, second slope and knot, which are usually called ‘growth factors’ and all together determine the functional form of the growth curve of  $\mathbf{y}_i$ .

=====  
 Insert Figure 1 about here  
 =====

We cannot fit the linear-linear piecewise change pattern specified in Equation (1) in the LGC framework for two reasons. First, the outcome variable  $y_{ij}$  does not have a unified pre- and post-knot expression. Second, the model in Equation (1) specifies a nonlinear relationship between the  $y_{ij}$  and the growth factor (or random coefficient in the mixed-effects model framework)  $\gamma_i$  and then cannot be estimated in the structural equation modeling (SEM) framework directly (Grimm et al., 2016b). Following Tishler and Zang (1981); Seber and Wild (2003); Grimm et al. (2016a); Liu (2019), the expression of repeated outcome in Equation (1) before and after the knot can be unified by reparameterization (see Appendix A.1 for details of reparameterization). We then write the repeated outcome as a linear combination of all four growth factors by the Taylor series expansion (Browne and du Toit, 1991; Grimm et al., 2016a; Liu, 2019) (see Appendix A.2 for details of Taylor series expansion). Accordingly, the model specified in Equation (1) can be written as a standard LGC model with reparameterized growth factors

$$\mathbf{y}_i = \mathbf{\Lambda}'_i(\gamma_i)\boldsymbol{\eta}'_i + \boldsymbol{\epsilon}_i, \quad (2)$$

where  $\mathbf{y}_i$  is a  $J \times 1$  vector of the repeated outcomes for the  $i^{th}$  person (in which  $J$  is the number of measurements),  $\boldsymbol{\eta}'_i$  is a  $4 \times 1$  vector of individual-level reparameterized growth factors and  $\mathbf{\Lambda}'_i(\gamma_i)$ , which is a function of time points and the unknown knot  $\gamma_i$ , is a  $J \times 4$  matrix of factor loadings. Additionally,  $\boldsymbol{\epsilon}_i$  is a  $J \times 1$  vector of residuals for the  $i^{th}$  person. For the  $i^{th}$  individual, the reparameterized growth factors (the measurement at the knot, the mean of two slopes, the half-difference of two slopes and the knot) and corresponding factor loadings are

$$\boldsymbol{\eta}'_i = \left( \eta'_{0i} \quad \eta'_{1i} \quad \eta'_{2i} \quad \delta_i \right)^T = \left( \eta_{0i} + \gamma_i\eta_{1i} \quad \frac{\eta_{1i} + \eta_{2i}}{2} \quad \frac{\eta_{2i} - \eta_{1i}}{2} \quad \gamma_i - \mu_\gamma \right)^T \quad (3)$$

and

$$\mathbf{\Lambda}'_i(\gamma_i) = \left( 1 \quad t_{ij} - \mu_\gamma \quad |t_{ij} - \mu_\gamma| \quad -\mu'_{\eta_2} - \frac{\mu'_{\eta_2}(t_{ij} - \mu_\gamma)}{|t_{ij} - \mu_\gamma|} \right) \quad (j = 1, \dots, J), \quad (4)$$

respectively, where  $\mu_\gamma$  is the knot mean and  $\delta_i$  is the deviation from the knot mean of the  $i^{th}$  individual. The reparameterized growth factors of the  $i^{th}$  individual can be further regressed on TICs,

$$\boldsymbol{\eta}'_i = \boldsymbol{\alpha}' + \mathbf{B}' \mathbf{X}_i + \boldsymbol{\zeta}'_i \quad (5)$$

where  $\boldsymbol{\alpha}'$  is a  $4 \times 1$  vector of reparameterized growth factor intercepts (which is the mean vector of reparameterized growth factors if the TICs are centered),  $\mathbf{B}'$  is a  $4 \times c$  matrix of regression coefficients (in which  $c$  is the number of TICs) from TICs to reparameterized growth factors,  $\mathbf{X}_i$ , which may either be continuous or be binary, is a  $c \times 1$  vector of covariates of the  $i^{th}$  individual, and  $\boldsymbol{\zeta}'_i$  is a  $4 \times 1$  vector of deviations of the  $i^{th}$  subject from the reparameterized growth factor means. To simplify estimation, we assume that the (reparameterized) growth factors are normally distributed conditional on individual-level covariates, so  $\boldsymbol{\zeta}'_i \sim \text{MVN}(\mathbf{0}, \boldsymbol{\Psi}'_\eta)$ , where  $\boldsymbol{\Psi}'_\eta$  is a  $4 \times 4$  unexplained variance-covariance matrix of reparameterized growth factors. We also assume that individual residuals,  $\epsilon_i$  in Equation (2), are identical and independent normal distribution over time, that is,  $\epsilon_i \sim \text{MVN}(\mathbf{0}, \theta_\epsilon \mathbf{I})$ , where  $\mathbf{I}$  is a  $J \times J$  identity matrix. Note that the intercepts and coefficients of reparameterized growth factors ( $\boldsymbol{\alpha}'$  and  $\mathbf{B}'$ ) as well as the unexplained growth factor variances  $\boldsymbol{\Psi}'_\eta$  no longer relate directly to the underlying developmental process and therefore lack meaningful, substantive interpretation. We demonstrate how to derive the coefficients in the original parameter-space so that all coefficients are interpretable.

## 2.2 Transformation Matrix and Inverse-transformation Matrix

When fitting a model, especially a complex model, in the SEM framework, selecting a proper set of initial values can improve the likelihood of convergence and then accelerate the computational process. Generally, descriptive statistics and visualization are tools for researchers to decide suitable initial values for the parameters of interest. However, it may not be straightforward for the reparameterized coefficients. Accordingly, the transformation matrices from parameters in the original frame to those in the reparameterized setting help decide appropriate initial values. More importantly, all reparameterized coefficients do not directly relate to the underlying change patterns and then need to be transformed back to be interpretable after estimating. So the inverse-transformation matrices that help derive the coefficients related to the underlying trajectory directly from the estimates are also needed.

Derived from Equation (3), the relationships between the original growth factors ( $\boldsymbol{\eta}_i$ ) and the reparameterized growth factors ( $\boldsymbol{\eta}'_i$ ) are  $\mathbf{G}_i$  and  $\mathbf{G}_i^{-1}$  for the  $i^{th}$  individual are given by

$$\begin{aligned} \boldsymbol{\eta}'_i &= \begin{pmatrix} \eta'_{0i} & \eta'_{1i} & \eta'_{2i} & \delta_i \end{pmatrix}^T = \begin{pmatrix} \eta_{0i} + \gamma_i \eta_{1i} & \frac{\eta_{1i} + \eta_{2i}}{2} & \frac{\eta_{2i} - \eta_{1i}}{2} & \gamma_i - \mu_\gamma \end{pmatrix}^T \\ &= \begin{pmatrix} 1 & \gamma_i & 0 & 0 \\ 0 & 0.5 & 0.5 & 0 \\ 0 & -0.5 & 0.5 & 0 \\ 0 & 0 & 0 & 1 \end{pmatrix} \begin{pmatrix} \eta_{0i} \\ \eta_{1i} \\ \eta_{2i} \\ \gamma_i - \mu_\gamma \end{pmatrix} = \mathbf{G}_i \times \begin{pmatrix} \eta_{0i} \\ \eta_{1i} \\ \eta_{2i} \\ \gamma_i - \mu_\gamma \end{pmatrix} \end{aligned}$$

and

$$\begin{aligned} \boldsymbol{\eta}_i &= \begin{pmatrix} \eta_{0i} & \eta_{1i} & \eta_{2i} & \gamma_i \end{pmatrix}^T = \begin{pmatrix} \eta'_{0i} - \gamma_i \eta'_{1i} + \gamma_i \eta'_{2i} & \eta'_{1i} - \eta'_{2i} & \eta'_{1i} + \eta'_{2i} & \delta_i + \mu_\gamma \end{pmatrix}^T \\ &= \begin{pmatrix} 1 & -\gamma_i & \gamma_i & 0 \\ 0 & 1 & -1 & 0 \\ 0 & 1 & 1 & 0 \\ 0 & 0 & 0 & 1 \end{pmatrix} \begin{pmatrix} \eta'_{0i} \\ \eta'_{1i} \\ \eta'_{2i} \\ \delta_i + \mu_\gamma \end{pmatrix} = \mathbf{G}_i^{-1} \times \begin{pmatrix} \eta'_{0i} \\ \eta'_{1i} \\ \eta'_{2i} \\ \delta_i + \mu_\gamma \end{pmatrix}. \end{aligned}$$

It is noted that the (inverse-) transformation matrix is individual-level due to the knot variance. For implementation, we employ the population-level (inverse-) transformation matrices to simplify the calculation. In Appendix A.3, we present the conditions under which the individual-level matrices can be approximated to be the population-level ones.

The transformation matrix and the inverse-transformation matrix between the mean vector of the original growth factors ( $\boldsymbol{\mu}_\eta$ ) and that of the reparameterized growth factors ( $\boldsymbol{\mu}'_\eta$ ) are

$$\boldsymbol{\mu}'_\eta \approx \begin{pmatrix} 1 & \mu_\gamma & 0 & 0 \\ 0 & 0.5 & 0.5 & 0 \\ 0 & -0.5 & 0.5 & 0 \\ 0 & 0 & 0 & 1 \end{pmatrix} \times \begin{pmatrix} \mu_{\eta_0} \\ \mu_{\eta_1} \\ \mu_{\eta_2} \\ 0 \end{pmatrix} = \mathbf{G} \times \begin{pmatrix} \mu_{\eta_0} \\ \mu_{\eta_1} \\ \mu_{\eta_2} \\ 0 \end{pmatrix}$$

and

$$\boldsymbol{\mu}_\eta \approx \begin{pmatrix} 1 & -\mu_\gamma & \mu_\gamma & 0 \\ 0 & 1 & -1 & 0 \\ 0 & 1 & 1 & 0 \\ 0 & 0 & 0 & 1 \end{pmatrix} \times \begin{pmatrix} \mu'_{\eta_0} \\ \mu_{\eta_1} \\ \mu_{\eta_2} \\ \mu_\gamma \end{pmatrix} = \mathbf{G}^{-1} \times \begin{pmatrix} \mu'_{\eta_0} \\ \mu_{\eta_1} \\ \mu_{\eta_2} \\ \mu_\gamma \end{pmatrix};$$

and those between the (unexplained) variance-covariance matrix of the original growth factors ( $\boldsymbol{\Psi}_\eta$ ) and that of the reparameterized growth factors ( $\boldsymbol{\Psi}'_\eta$ ) are

$$\begin{aligned} \boldsymbol{\Psi}'_\eta &\approx E(\text{Var}(\mathbf{G}_i \times \boldsymbol{\eta}_i | \gamma_i)) = E(\nabla \mathbf{G}_i \text{Var}(\boldsymbol{\eta}_i) \nabla \mathbf{G}_i^T) \\ &\approx \begin{pmatrix} 1 & \mu_\gamma & 0 & \mu_{\eta_1} \\ 0 & 0.5 & 0.5 & 0 \\ 0 & -0.5 & 0.5 & 0 \\ 0 & 0 & 0 & 1 \end{pmatrix} \boldsymbol{\Psi}_\eta \begin{pmatrix} 1 & \mu_\gamma & 0 & \mu_{\eta_1} \\ 0 & 0.5 & 0.5 & 0 \\ 0 & -0.5 & 0.5 & 0 \\ 0 & 0 & 0 & 1 \end{pmatrix}^T \\ &= \nabla \mathbf{G} \boldsymbol{\Psi}_\eta \nabla \mathbf{G}^T \end{aligned}$$

and

$$\begin{aligned} \boldsymbol{\Psi}_\eta &\approx E(\text{Var}(\mathbf{G}_i^{-1} \times \boldsymbol{\eta}'_i | \gamma_i)) = E(\nabla \mathbf{G}_i^{-1} \text{Var}(\boldsymbol{\eta}'_i) \nabla \mathbf{G}_i^{-1T}) \\ &\approx \begin{pmatrix} 1 & -\mu_\gamma & \mu_\gamma & 0 \\ 0 & 1 & -1 & 0 \\ 0 & 1 & 1 & 0 \\ 0 & 0 & 0 & 1 \end{pmatrix} \boldsymbol{\Psi}'_\eta \begin{pmatrix} 1 & -\mu_\gamma & \mu_\gamma & 0 \\ 0 & 1 & -1 & 0 \\ 0 & 1 & 1 & 0 \\ 0 & 0 & 0 & 1 \end{pmatrix}^T \\ &= \nabla \mathbf{G}^{-1} \boldsymbol{\Psi}'_\eta \nabla \mathbf{G}^{-1T}. \end{aligned}$$

When regressing growth factors on the individual-level covariates as we did in Equation (5), we also need to reparameterize the growth factor intercepts and path coefficients. We center the covariates to simplify the calculation. On the one hand, the vector  $\boldsymbol{\alpha}'$  is equivalent to the mean vector of the reparameterized growth factor ( $\boldsymbol{\mu}'_\eta$ ) when all covariates are centered. Accordingly, the transformation and inverse-transformation matrices between the original intercepts ( $\boldsymbol{\alpha}$ ) and the reparameterized intercepts ( $\boldsymbol{\alpha}'$ ) are  $\mathbf{G}$  and  $\mathbf{G}^{-1}$ , respectively. On the other hand, through centering the covariates, we simplify the transformation and inverse-transformation matrices between the original path coefficients ( $\mathbf{B}$ ) and the reparameterized path coefficients ( $\mathbf{B}'$ ) as  $\nabla \mathbf{G}$  and  $\nabla \mathbf{G}^{-1}$ , respectively. The detailed derivation is shown in Appendix A.4.

When fitting the model using software such as the *R* package *OpenMx*, which allows for matrix calculation on those estimates from the model by the function *mxAlgebra()* (Boker et al., 2018), we only need to provide the matrices  $\mathbf{G}^{-1}$  and  $\nabla \mathbf{G}^{-1}$ , and the package can derive the coefficients in the original setting automatically. Specifically, we need to specify the inverse-transformation matrices, the estimated mean vector and variance-covariance structure of reparameterized growth factors, and the algebraic expression (i.e., matrix multiplication) between them in the function *mxAlgebra()*. *OpenMx* can calculate the point estimates with their standard errors of the growth factor coefficients in the original setting. Other SEM software such as *Mplus* can also calculate new parameters to be derived from those estimated automatically by specifying their relationship in the *NEW* command. However, we need to derive the expression for each cell of the mean vector and the variance-covariance matrix of the original growth factors since *Mplus* does not allow for matrix algebra. All these expressions are in Appendix A.5.

### 2.3 Model Estimation

For the  $i^{\text{th}}$  individual, the expected mean vector and the variance-covariance structure of the repeated measurements of the model given in Equations (2) and (5) can be expressed as

$$\boldsymbol{\mu}_i = \boldsymbol{\Lambda}'_i(\gamma_i)(\boldsymbol{\alpha}' + \mathbf{B}' \boldsymbol{\mu}_X) \quad (6)$$

and

$$\boldsymbol{\Sigma}_i = \boldsymbol{\Lambda}'_i(\gamma_i) \boldsymbol{\Psi}'_\eta \boldsymbol{\Lambda}'_i(\gamma_i)^T + \boldsymbol{\Lambda}'_i(\gamma_i) \mathbf{B}' \boldsymbol{\Phi} \mathbf{B}'^T \boldsymbol{\Lambda}'_i(\gamma_i)^T + \theta_\epsilon \mathbf{I}, \quad (7)$$

where  $\boldsymbol{\mu}_X$  and  $\boldsymbol{\Phi}$  are the mean vector ( $c \times 1$ ) and the variance-covariance matrix ( $c \times c$ ) of the TICs, respectively.

The parameters in the model given in Equations (2) and (5) include the mean vector and unexplained variance-covariance matrix of reparameterized growth factors, the re-expressed path coefficients as well as the means and the variance-covariance structure of covariates. Then by the inverse-transformation matrices provided in Section 2.2, the parameters

in the original setting can be calculated.  $\Theta_1$  and  $\Theta'_1$  in Equations

$$\begin{aligned}\Theta_1 &= \{\alpha, \Psi_\eta, \mathbf{B}, \mu_X, \Phi, \theta_\epsilon\} \\ &= \{\mu_{\eta_0}, \mu_{\eta_1}, \mu_{\eta_2}, \mu_\gamma, \psi_{00}, \psi_{01}, \psi_{02}, \psi_{0\gamma}, \psi_{11}, \psi_{12}, \psi_{1\gamma}, \psi_{22}, \psi_{2\gamma}, \psi_{\gamma\gamma}, \mathbf{B}, \mu_X, \Phi, \theta_\epsilon\}\end{aligned}$$

and

$$\begin{aligned}\Theta'_1 &= \{\alpha', \Psi'_\eta, \mathbf{B}', \mu_X, \Phi, \theta_\epsilon\} \\ &= \{\mu'_{\eta_0}, \mu'_{\eta_1}, \mu'_{\eta_2}, \mu_\gamma, \psi'_{00}, \psi'_{01}, \psi'_{02}, \psi'_{0\gamma}, \psi'_{11}, \psi'_{12}, \psi'_{1\gamma}, \psi'_{22}, \psi'_{2\gamma}, \psi'_{\gamma\gamma}, \mathbf{B}', \mu_X, \Phi, \theta_\epsilon\}\end{aligned}$$

list the parameters in the original and reparameterized frames, respectively.

We then use full information maximum likelihood (FIML) to estimate  $\Theta'_1$  due to the potential heterogeneity of individual contributions to the likelihood. The log-likelihood function of each individual and that of the overall sample can be expressed as

$$\log lik_i(\Theta'_1 | \mathbf{y}_i) = C - \frac{1}{2} \ln |\Sigma_i| - \frac{1}{2} (\mathbf{y}_i - \mu_i)^T \Sigma_i^{-1} (\mathbf{y}_i - \mu_i), \quad (8)$$

and

$$\log lik(\Theta'_1) = \sum_{i=1}^n \log lik_i(\Theta'_1 | \mathbf{y}_i), \quad (9)$$

respectively, where  $C$  is a constant,  $n$  is the number of individuals,  $\mu_i$  and  $\Sigma_i$  are the mean vector and the variance-covariance matrix of  $\mathbf{y}_i$ , which have been defined in Equations (6) and (7), respectively. We construct the full model using the R package *OpenMx* with the optimizer CSOLNP (Neale et al., 2016; Pritikin et al., 2015; Hunter, 2018; Boker et al., 2018), with which we are able to fit the model and implement the (inverse-) transformation matrices as shown in Section 2.2 efficiently.

## 2.4 Reduced Model

With an assumption that the change-point is roughly similar for each individual, we can fix the between-individual differences in the knot to 0 and construct a reduced model to estimate a knot without considering variability. We can specify the reduced model as

$$\begin{aligned}\mathbf{y}_i &= \Lambda'_i(\gamma) \eta'_i + \epsilon_i, \\ \eta'_i &= \alpha' + \mathbf{B}' \mathbf{X}_i + \zeta'_i,\end{aligned}$$

where  $\eta'_i$  is a  $3 \times 1$  vector of reparameterized growth factor (the measurement of the knot, the mean of two slopes, and the half-difference of two slopes), and  $\Lambda_i(\gamma)$ , a function of time points and a fixed change-point  $\gamma$ , is a  $J \times 3$  matrix of factor loadings. We can further express the reparameterized growth factors and corresponding factor loadings as

$$\eta'_i = \begin{pmatrix} \eta'_{0i} & \eta'_{1i} & \eta'_{2i} \end{pmatrix}^T = \begin{pmatrix} \eta_{0i} + \gamma \eta_{1i} & \frac{\eta_{1i} + \eta_{2i}}{2} & \frac{\eta_{2i} - \eta_{1i}}{2} \end{pmatrix}^T$$

and

$$\Lambda'_i(\gamma) = \begin{pmatrix} 1 & t_{ij} - \gamma & |t_{ij} - \gamma| \end{pmatrix} \quad (j = 1, \dots, J).$$

The growth factor intercepts  $\alpha'$ , path coefficients  $\mathbf{B}'$  and the deviation  $\zeta'_i$  of the  $i^{th}$  individual from the reparameterized growth factor means also reduced to be a  $3 \times 1$  vector,  $3 \times c$  matrix and  $3 \times 1$  vector, respectively. The transformation and inverse-transformation matrices are also reduced accordingly. Specifically, we only need the first three rows and the first three columns in the matrices  $\mathbf{G}$ ,  $\mathbf{G}^{-1}$ ,  $\nabla \mathbf{G}$  and  $\nabla \mathbf{G}^{-1}$ , since only three growth factors need to be reparameterized. Note that the population-level (inverse-) transformation matrices are the same as the individual-level (inverse-) transformation matrices for the reduced model.

For the  $i^{th}$  individual, the expected mean vector and the variance-covariance matrix of the repeated outcomes of this model are

$$\mu_i = \Lambda'_i(\gamma) (\alpha' + \mathbf{B}' \mu_X) \quad (10)$$

and

$$\Sigma_i = \Lambda'_i(\gamma) \Psi'_\eta \Lambda'_i(\gamma)^T + \Lambda'_i(\gamma) \mathbf{B}' \Phi \mathbf{B}'^T \Lambda'_i(\gamma)^T + \theta_\epsilon \mathbf{I}, \quad (11)$$

respectively. For this reduced model,  $\Theta_2$  and  $\Theta'_2$  are defined as

$$\begin{aligned}\Theta_2 &= \{\alpha, \gamma, \Psi_\eta, \mathbf{B}, \mu_X, \Phi, \theta_\epsilon\} \\ &= \{\mu_{\eta_0}, \mu_{\eta_1}, \mu_{\eta_2}, \gamma, \psi_{00}, \psi_{01}, \psi_{02}, \psi_{11}, \psi_{12}, \psi_{22}, \mathbf{B}, \mu_X, \Phi, \theta_\epsilon\}\end{aligned}$$

and

$$\begin{aligned}\Theta'_2 &= \{\alpha', \gamma, \Psi'_\eta, \mathbf{B}', \boldsymbol{\mu}_X, \Phi, \theta_\epsilon\} \\ &= \{\mu'_{\eta_0}, \mu'_{\eta_1}, \mu'_{\eta_2}, \gamma, \psi'_{00}, \psi'_{01}, \psi'_{02}, \psi'_{11}, \psi'_{12}, \psi'_{22}, \mathbf{B}', \boldsymbol{\mu}_X, \Phi, \theta_\epsilon\},\end{aligned}$$

and list the parameters in the original and reparameterized setting, respectively. By replacing  $\Theta'_1$  in Equations (8) and (9) with  $\Theta'_2$  and updating  $\boldsymbol{\mu}_i$  and  $\boldsymbol{\Sigma}_i$  as such defined in Equations (10) and (11), we have the likelihood function of each individual and that of the overall sample. We build the reduced model using the R package *OpenMx* with the optimizer CSOLNP and employ the FIML technique to estimate the parameters. We provide the *OpenMx* syntax for the full model and its reduced version as well as a demonstration in the online appendix ([https://github.com/Veronica0206/Dissertation\\_projects](https://github.com/Veronica0206/Dissertation_projects)). For the researchers who are interested in using *Mplus*, we also provide *Mplus* 8 syntax for both models in the online appendix.

### 3 Model Evaluation

The proposed method was evaluated using a Monte Carlo simulation study with two goals. The first goal was to evaluate how the approximation led by the Taylor series expansion and replacing the individual-level with the population-level inverse-transformation matrices affected the estimating effects, including the relative bias, the empirical standard error (SE), the relative root-mean-square error (RMSE), and the empirical coverage probability for a nominal 95% confidence interval of each parameter. We provide the definitions and estimates of these four performance metrics in Table 1. The second goal was to examine how the reduced model performed as a parsimonious backup of the full model.

=====  
 Insert Table 1 about here  
 =====

In the simulation study, we followed Morris et al. (2019) and decided the number of replications  $S = 1,000$  by an empirical approach. We conducted a pilot simulation run and found that standard errors of all coefficients except the unexplained intercept variance (i.e.,  $\psi_{00}$ ) were less than 0.15. As the most important performance metric in the simulation study was the (relative) bias and we wanted to keep its Monte Carlo standard error<sup>2</sup> lower than 0.005, we needed at least 900 replications. We then decided to proceed with  $S = 1,000$  for more conservative consideration.

#### 3.1 Design of Simulation Study

As mentioned earlier, the parameters of the most interest in the full model are the knot, its variance and the path coefficients to the knot. The conditions hypothesized to influence the estimation of these knot parameters, along with other model parameters, included sample size, the number of repeated measurements, the knot locations, the knot variances, shapes of trajectories, measurement precision, and the proportion of growth factor variances explained by time-invariant covariates. Accordingly, we did not investigate some conditions that were assumed would not affect the model performance meaningfully. For instance, the mean vector and variance-covariance matrix of the first three growth factors (i.e., the intercept and two slopes) usually change with the measurement scale and time scale in practice. As shown in Table 2, accordingly, we fixed the mean of intercept and first slope and only changed that of the second slope. We also fixed the variance-covariance matrix of the first three growth factors and kept the index of dispersion ( $\sigma^2/\mu$ ) of each at a tenth scale, guided by previous simulation studies for growth models (Bauer and Curran, 2003; Kohli, 2011; Kohli et al., 2015b). Further, the growth factors were set to be positively correlated to a moderate degree ( $\rho = 0.3$ ).

=====  
 Insert Table 2 about here  
 =====

We list all conditions that we considered in the simulation design in Table 2. For a model to analyze longitudinal data, the factor that we are most interested in is the number of repeated measures. Generally, the model should perform better if the study duration is longer, which we wanted to investigate by the simulation study. Another important factor for the linear-linear trajectory is the knot location. Intuitively, the model should perform the best if we let the knot in the middle of study duration; we were interested in testing this hypothesis. Accordingly, we chose two different levels of the number of measurements: 6 and 10. We selected 6 as the minimum number of repeated outcomes to

---

<sup>2</sup>Monte Carlo SE(Bias) =  $\sqrt{Var(\hat{\theta})/S}$  (Morris et al., 2019).

make the full model fully identified<sup>3</sup>. For the conditions with 6 repeated measures, we set the knot at halfway of study duration ( $\mu_\gamma = 2.5$ ). The other level 10 was considered for two reasons. First, we wanted to evaluate whether a more extended study duration would improve model performance. More importantly, 10 measurements allowed us to place knots at different locations, say the halfway knot ( $\mu_\gamma = 4.5$ ) as well as a left-shifted knot ( $\mu_\gamma = 3.5$ ) and right-shifted knot ( $\mu_\gamma = 5.5$ ) from the middle point of study duration. Around each wave, we allowed a time-window with width  $(-0.25, +0.25)$ , which is a ‘medium’ deviation as Coulombe et al. (2015), for individual measurement occasions.

In order to fit the full model in the SEM framework and obtain interpretable coefficients, the approximation was introduced by the Taylor series expansion and replacing the individual-level with the population-level inverse-transformation matrices. As shown in Appendix A.2 and A.3, the essential conditions to apply the Taylor series expansion and use the population-level matrices is that the knot variance approaches to 0. We then investigated 3 levels of magnitude of between-person differences in the knot to evaluate how the introduced approximation affects the model performance and compare the full model to the reduced model. We set the knot standard deviation as 0, 0.3 and 0.6 as the zero, medium and large difference in the knot location. Note that the magnitude of the knot is relative to the scale of measurement occasions.

Additionally, we examined how the shape of change patterns, which was quantified by the standardized difference between two slopes, affects the full model. It is noted that we considered both positive and negative differences ( $\eta_1 < \eta_2$  and  $\eta_1 > \eta_2$ , respectively) to assess model performance in the two cases as shown in Figure A.1. For each case, we considered 3 levels of standardized difference between two slopes to evaluate the models. We also considered two levels of effects of exogenous variables on endogenous growth factors<sup>4</sup>, two levels of sample size, and two levels of measurement precision as shown in Table 2.

### 3.2 Data Generation and Simulation Step

For each condition which is listed in Table 2, the general steps of the simulation study for the models were carried out as follows:

1. Generated data for growth factors and TICs simultaneously using the R package *MASS* (Venables and Ripley, 2002) (details are provided in Appendix A.6),
2. Generated the time structure with  $J$  scaled and equally-spaced waves  $t_j$  and obtained ITPs:  $t_{ij} \sim U(t_j - \Delta, t_j + \Delta)$  by allowing disturbances around each wave,
3. Calculated factor loadings, which are functions of ITPs and the knot, for each individual,
4. Calculated values of the repeated measurements based on growth factors, factor loadings, and residual variances.
5. Implemented the full model and its reduced form on simulated data, estimated the parameters, constructed corresponding 95% Wald CIs,
6. Replicated the above steps until after obtaining 1,000 convergent solutions.

## 4 Result

### 4.1 Model Convergence and Proper Solution

In this section, we first examined the convergence rate and component fit measures of each condition. The convergence<sup>5</sup> rate of each condition was investigated. Based on our simulation studies, the full model and its reduced version converged satisfactorily (the convergence rate of the full model achieved at least 90% while that of the reduced model was 100%). Out of a total of 576 conditions, 490 conditions reported 100% convergence rate and 67 conditions reported convergence rate of 99% to 100%. The worst scenario in terms of the non-convergence rate across all conditions was 46/1046, indicating that we needed to repeat the steps described in Section 3.2 1,046 times to have 1,000 replications with a convergent solution. It occurred under the condition with the smaller sample size (i.e.,  $n = 200$ ), the shorter study duration (i.e.,  $J = 6$ ), less precise measurements (i.e.,  $\theta_\epsilon = 2$ ), the largest knot standard deviation (i.e.,  $sd(\gamma) = 0.6$ ), and the smallest positive standardized difference between two slopes (i.e.,  $d_z + 1$ ).

<sup>3</sup>Although the information of model identification of linear-linear growth model with an unknown knot lacks, it has been proved that the bilinear latent growth model can be identified with at least five waves with a specified knot at the halfway of study duration (Bollen and Curran, 2005).

<sup>4</sup>We let the TICs explain moderate (13%) and substantial (26%) variances of such factors (Cohen, 1988).

<sup>5</sup>In our project, convergence is defined as to achieve *OpenMx* status code 0, which suggests a successful optimization, until up to 10 attempts with different sets of starting values (Neale et al., 2016).

We also conducted diagnostics to investigate improper solutions, such as estimates of growth factor variances that are less than 0, and/or estimates of correlations between growth factors are beyond  $[-1, 1]$ . Table 3 demonstrates the number of improper solutions yielded by the full model under conditions with 10 repeated measures, the knot midway through the total time of observation, and 13% explained variance of the latent growth factors, which include negative knot variances and its out-of-range (i.e., out of  $[-1, 1]$ ) correlations with any other growth factors. When the population value of the knot variance was 0 or relatively small (i.e.,  $sd(\gamma) = 0.3$ ), the number of improper solutions was relatively large.

=====  
 Insert Table 3 about here  
 =====

For the scenarios including knots with variability, we observed that the proper solution rate has positive associations with the magnitude of standardized difference, the measurement precision, the sample size, and the knot standard deviation. The sign of  $d_z$  seemed not to affect the number of improper solution meaningfully. However, the shifted knot locations or the proportion of explained variance of growth factors did not affect the rate of improper solution meaningfully but that reduced follow-up time inflated this number. When such improper solutions emerged, we replaced the full model with its reduced version for the model evaluation.

## 4.2 Estimating Effects

In this section, we present simulation results in terms of estimating effects, which include the relative bias, empirical SE, relative RMSE and empirical coverage probability for a nominal 95% confidence interval for each parameter of interest. Generally, the full model estimates coefficients unbiasedly, precisely, and exhibiting appropriate confidence interval coverage. We first provide the summary statistics (specifically, median and range) for each performance metric of each parameter across the conditions with 10 repeated measurements and the midway knot. Then we discuss how the simulation conditions affect these performance metrics.

Tables 4 and 5 present the median (range) of the relative bias and empirical SE, respectively, for each parameter of interest across all conditions with 10 repeated measurements and the halfway knot for the full model and its reduced version. We first calculated the relative bias/empirical SE of each parameter across 1,000 replications under each condition and then summarized the relative biases/empirical SEs of each parameter over all aforementioned conditions as the median (range) of relative bias/empirical SE. As shown in Tables 4 and 5, both models generated unbiased point estimates with small empirical SEs generally, and the full model performed better than its reduced version as the ranges of relative biases of the parameters from the full model were narrower than those from the reduced model. Specifically, for the full model, the magnitude of relative biases of the growth factor means was under 0.03, that of path coefficients to the intercept and two slopes was under 0.12, and that of unexplained variances of the intercept and two slopes was under 0.07. From Table 4, the full model may produce biased estimates for the knot variances and the path coefficients to the knot: the median values of relative biases of  $\beta_{1\gamma}$ ,  $\beta_{2\gamma}$  and  $\psi_{\gamma\gamma}$  were  $-0.2712$ ,  $-0.2709$  and  $0.0403$ , respectively.

=====  
 Insert Table 4 about here  
 =====

=====  
 Insert Table 5 about here  
 =====

We plotted the relative bias under each condition with 10 repeated measures and the midway knot for  $\psi_{\gamma\gamma}$ ,  $\beta_{1\gamma}$  and  $\beta_{2\gamma}$  in Figure 2 to further investigate the relative bias pattern for the knot variance and the path coefficients to the knot. From the figure, we observed how the conditions we set up in the simulation design affected these estimates. First, under the conditions where the knot standard deviation was 0.3 and/or the standardized difference between two slopes was medium or large (i.e.,  $d_z = 1.5$  or  $d_z = 2.0$ ), estimates were less biased. Second, the unexplained knot variance,  $\psi_{\gamma\gamma}$ , was underestimated under the conditions with 0.6 knot standard deviation while overestimated under the conditions with 0.3 knot standard deviation, and the path coefficients to the knot (i.e.,  $\beta_{1\gamma}$  and  $\beta_{2\gamma}$ ) were underestimated under all investigated conditions. Third, other conditions, such as the sample size or the proportion of growth factor variance explained by the covariates, did not influence the relative biases meaningfully.

=====  
 Insert Figure 2 about here  
 =====

From Table 5, estimates from the full model and its reduced version were precise: the magnitude of empirical standard errors of slope or knot parameters were around 0.10, although those values of intercept parameters were relatively large: the empirical standard error of the intercept mean, and that of the unexplained intercept variance achieved 0.35 and 2.35, respectively.

Table 6 lists the median (range) of relative RMSE of each parameter for both models under the conditions with 10 repeated measures and the midway knot, which combines bias and precision to examine the model performance holistically. From the table, both models estimated parameters accurately. The magnitude of relative RMSEs of growth factor means was under 0.05, and the median RMSE value of path coefficients to the intercept or slopes was around 0.20.

=====  
 Insert Table 6 about here  
 =====

Table 7 presents the median (range) of the coverage probability (CP) for the full model and its reduced version under the conditions with 10 repeated measurements and the midway knot. Under the majority conditions, the full model performed well in terms of empirical coverage as the median values of coverage probabilities of all parameters were around 0.95. We noticed that the coverage probabilities of knot variance and path coefficients to the knot could be conservative under the conditions with 0.6 knot standard deviation.

=====  
 Insert Table 7 about here  
 =====

To sum up, based on our simulation study, the estimates from the full model were unbiased and precise, with proper 95% coverage probabilities generally. As pointed out earlier, the essential conditions for applying the Taylor series expansion and using the population-level inverse-transformation matrices is that the knot variance approaches 0. Through the simulation study, we found that the full model worked well under the conditions with the medium level of knot standard deviation (i.e.,  $sd(\gamma) = 0.3$  for the scaled measurement occasions) though less satisfactory when the knot standard deviation was large. Additionally, some factors, for example, sample size and measurement precision, influenced model performance. Specifically, the larger sample size (i.e.,  $n = 500$ ) and more precise measurement ( $\theta_\epsilon = 1$ ) improved estimating effects. The trajectory shape quantified by the standardized difference between two slopes affected the estimating effects shown in Figure 2. We also examined the model performance under the conditions which were not summarized in Tables 4, 5, 6 and 7 and found that shorter study duration (i.e.,  $J = 6$ ) and left- (right-) shifted knot locations only affected the estimating effects slightly.

## 5 Application

This section demonstrates the use of the full model to approximate nonlinear trajectories and estimate a knot that varies across individuals. This application had two goals. The first goal was to compare the fitness of bilinear spline functional form to three common parametric change patterns: linear, quadratic and Jenss-Bayley growth curve. The second goal was to show how to select the model between the full model and the reduced version. We randomly selected 400 students from the Early Childhood Longitudinal Study Kindergarten Cohort: 2010-11 (ECLS-K: 2011) with complete records of repeated mathematics IRT scaled scores, demographic information (sex, race, and age at each wave), school information (baseline school location and baseline school type), and social-economic status (baseline family income and the highest education level between parents)<sup>6</sup>.

ECLS-K: 2011 is a nationally representative longitudinal sample of US children enrolled in about 900 kindergarten programs starting from 2010 – 2011 school year. Children’s mathematics ability was assessed in nine waves: fall and spring of kindergarten (2010 – 2011), first (2011 – 2012) and second (2012 – 2013) grade, respectively, as well as spring of 3<sup>rd</sup> (2014), 4<sup>th</sup> (2015) and 5<sup>th</sup> (2016), respectively. Only about 30% students were sampled in the fall of 2011 and 2012 (Lê et al., 2011). Noting that two possible time scales are available in the data set: students’ age and their grade-in-school, we decided to use children’s age (in months) to have individual measurement occasions in the main analysis and conduct a sensitivity analysis where students’ grade-in-school was used as the time scale. In the subsample, 51% of children were male, and 49% of children were female. Additionally, 45% of students were White, 5% were Black, 38% were Hispanic, 8% were Asian, and 4% were others. For this analysis, we dichotomized the

<sup>6</sup>The total sample size of ECLS-K: 2011 is  $n = 18174$ . The number of entries after removing records with missing values (i.e., rows with any of NaN/-9/-8/-7/-1) is  $n = 2290$ .

variable race to be White (45%) and others (55%). At the start of the study, 11% and 89% students were in private and public school, respectively; 31%, 50%, 4% and 16% students were from a school located in city, suburb, town and rural areas, respectively. We treated the variable the highest parents' education (ranged between 0 and 8) and family income (ranged between 1 and 18) as continuous variables, and corresponding mean (SD) was 5.18 (2.10) and 11.56 (5.42), respectively.

## Main Analysis

In this section, we use children's age (in months) as the time metric to have individual measurement occasions. We first fit the full and reduced linear-linear piecewise models as well as three parametric growth curve functions, linear, quadratic and Jenss-Bayley. The graphical representations of the model implied curves on the smooth line of the observed mathematics IRT scores are shown in Figure 3. From the figure, the nonlinear functional forms fit better than the linear function generally; and the models with bilinear spline change patterns fit better than the parametric nonlinear models to the first two or three measurement occasions. As shown in Figure 3, both the quadratic growth curve and the Jenss-Bayley tended to underestimate the mathematics achievement in the early stage.

=====  
 Insert Figure 3 about here  
 =====

Table 8 provides the obtained estimated likelihood, information criteria (including AIC and BIC), residuals of each latent growth curve model. From the table, the model with the linear-linear functional form and a random knot has the largest estimated likelihood, smallest AIC and smallest residual though its BIC is slightly larger than the LGC with the quadratic function. Moreover, from Table 8, the full model consistently performs better than its reduced version for this empirical example, indicating that we need to consider the variability of the knot, although the model implied trajectory of both captures the overall observed data well as shown in Figure 3. We then fit the full model to investigate the impact of covariates, such as sex, race, parents' highest education (baseline), family income (baseline), school type (baseline), and school location (baseline), have on the knot variance (and other growth factor variances). Its model fit information is also provided in Table 8.

=====  
 Insert Table 8 about here  
 =====

Table 9 presents the estimates of parameters of interest. It is noticed that post-knot development in mathematics skills slowed down substantially (on average 1.731 and 0.689 per month in the pre- and post-knot stage, respectively). The knot was estimated at 102 month on average (8.5-years old). We noted that the initial mathematics performance (60-month old in our case) was positively associated with family income, private school, and parents' highest education. Moreover, the family income also can explain the individual difference in the development rate of mathematics IRT scores in the first stage. Further, boys improved more rapidly than girls in terms of mathematics ability in the first stage. Additionally, children coming from schools in rural areas arrived at the change-point later.

=====  
 Insert Table 9 about here  
 =====

## Sensitivity Analysis

In this section, we use students' grade-in-school as the time scale, where the time metric takes on discrete values (for example, 0 is for the kindergarten fall semester, and 0.5 in years or 6 in months is for the kindergarten spring semester). We list the estimated likelihood, AIC, BIC, and the residual variance of the linear-linear piecewise growth model in Table 8<sup>7</sup>. Upon further examination, the mathematics ability slowed down between the sixth and the seventh wave (around the fall semester of Grade 3), matching the estimate in the main analysis: students in Grade 3 usually aged between 8- to 9-year old. The effect size of the estimates of the path coefficients to the knot increased slightly, but the direction of the estimates kept the same.

<sup>7</sup>Note that the model constructed in the sensitivity analysis cannot be compared with that for that in the main analysis directly since the raw data sets used in the two parts were different.

## 6 Discussion

In this article, we proposed (inverse-) transformation matrices for the linear-linear piecewise growth curve model with an unknown random knot to obtain interpretable parameters. We extended the existing model to the framework of individual measurement occasions to account for the heterogeneity of the measurement time. More importantly, we conducted intensive simulation studies to demonstrate that the model performed well under the conditions with a medium level knot standard deviation, which aligns with the essential condition to use the Taylor series expansion and the population-level transformation matrices. We proposed using a parsimonious model with the assumption that the knot location of all individuals is roughly at the same time point. Based on the simulation results, we recommend employing the reduced model, which only estimates the knot itself if the full model fails to converge or generates improper solutions or the knot variance is out of research interest.

The (inverse-) transformation matrices between growth factors in two parameter-spaces are valuable for the reparameterizing longitudinal model. One drawback of the reparameterizing longitudinal model initially was that the reparameterized coefficients no longer relate to the underlying developmental process and therefore lack meaningful, substantive interpretation, thus requiring a back transformation of the model parameters. In the linear-linear piecewise growth model with an unknown random knot, this transformation is individual-level as each individual has a ‘personal’ knot. We then proposed to use the population-level (inverse-) transformation matrices to simplify the calculation. The matrix form is especially convenient when we use the *R* package *OpenMx* that allows for matrix algebra. The transformation matrices for other reparameterizing longitudinal models can also be proposed.

We introduced approximation when applying the Taylor series expansion (to obtain the factor loadings of the knot, an additional growth factor) and replacing the individual-level with the population-level transformation matrices (to simplify the calculation). Intensive simulation studies were conducted and demonstrated that the model worked satisfactorily if the knot standard deviation is not too large, which aligns with our initial hypothesis. Under the conditions with a large knot standard deviation, the model for estimating a random knot was less satisfactory, but it still was better than the reduced version.

In this study, we extended the linear-linear piecewise growth model to the framework of individual measurement occasions to account for possible heterogeneity in measurement time. To demonstrate the influence of the time scale has on the estimates, we conducted a sensitivity analysis in the application section. The fixed effects of growth factors obtained from the model with different time scales were matched, though the estimated effect size of path coefficients increased when we used the grade-in-school as the time scale. This difference is not surprising as students in the same grade-in-school could be of different ages. In practice, we recommend selecting the time scale by research questions instead of any statistical criteria.

We demonstrated the use of the proposed method on a subset with  $n = 400$  from ECLS-K: 2011 with a hope to show the procedure and provide a set of recommendations for possible issues that researchers may face in a real-world data analysis. First of all, we recommend selecting a proper functional form to depict trajectories before identifying the possible time-invariant covariates to explain the between-individual difference in the within-individual change, though this selection is not straightforward. Many factors, such as the research question, the fit between the model implied and the observed trajectory, and the information criteria, drive this selection process. It is worth considering either the full or the reduced model to estimate the knot if it is the research interest. If the interest lies in to fit nonlinear trajectories, it may be appropriate to fit the change patterns with several functional forms and then select the ‘best’ one. It is noted that the fit information, sometimes, fails to lead unequivocal selection as in our empirical example. Although either the full model or the quadratic functional forms can be viewed as an ‘acceptable’ model, the full model is better if it is important to capture children’s mathematics achievement in the early stage of the study. The selection between the full and the reduced model can only rely on the information criteria such as the BIC as they usually fit the trajectories equally, as shown in Figure 3.

In this article, we focused on the growth model with a bilinear spline functional form because it is the most straightforward and intuitive but useful. It can be generalized to a linear spline with multiple knots or a nonlinear spline (such as a linear-polynomial piecewise), where the corresponding (inverse-) transformation matrices can also be derived. Besides, it is accessible to extend the current work to address longitudinal studies with dropout under the assumption of missing at random thanks to the FIML technique. Moreover, we introduced approximations when replacing the individual-level inverse-transformation matrices with the population-level inverse-transformation matrices. The individual-level inverse-transformation matrices are also realizable with a more complicated process if more unbiased and precise estimates are desirable. Additionally, we focused on time-invariant covariates in the current work, which is helpful to identify baseline characteristics to explain the variability of growth factors. It can also be extended to investigate time-varying covariates to explain the individual-difference in the trajectories.

## Appendix A Formula Derivation

### A.1 The Reparameterizing Procedure for Growth Factors

Tishler and Zang (1981) and Seber and Wild (2003) showed that the bilinear spline regression model can be written as either the minimum or maximum response value of two trajectories. By extending such expressions to the LGC framework, two forms of bilinear spline for the  $i^{th}$  individual are shown in Figure A.1. In the left panel ( $\eta_{1i} > \eta_{2i}$ ), the measurement  $y_{ij}$  should always be the minimum value of two lines; that is,  $y_{ij} = \min(\eta_{0i} + \eta_{1i}t_{ij}, \eta_{02i} + \eta_{2i}t_{ij})$ . To unify the expression of measurements pre- and post-knot, we have the following equation

$$\begin{aligned}
y_{ij} &= \min(\eta_{0i} + \eta_{1i}t_{ij}, \eta_{02i} + \eta_{2i}t_{ij}) \\
&= \frac{1}{2}(\eta_{0i} + \eta_{1i}t_{ij} + \eta_{02i} + \eta_{2i}t_{ij} - |\eta_{0i} + \eta_{1i}t_{ij} - \eta_{02i} - \eta_{2i}t_{ij}|) \\
&= \frac{1}{2}(\eta_{0i} + \eta_{1i}t_{ij} + \eta_{02i} + \eta_{2i}t_{ij}) - \frac{1}{2}(|\eta_{0i} + \eta_{1i}t_{ij} - \eta_{02i} - \eta_{2i}t_{ij}|) \\
&= \frac{1}{2}(\eta_{0i} + \eta_{02i} + \eta_{1i}t_{ij} + \eta_{2i}t_{ij}) - \frac{1}{2}(\eta_{1i} - \eta_{2i})|t_{ij} - \gamma_i| \\
&= \eta'_{0i} + \eta'_{1i}(t_{ij} - \gamma_i) + \eta'_{2i}|t_{ij} - \gamma_i| \\
&= \eta'_{0i} + \eta'_{1i}(t_{ij} - \gamma_i) + \eta'_{2i}\sqrt{(t_{ij} - \gamma_i)^2},
\end{aligned} \tag{A.1}$$

where  $\eta'_{0i}$ ,  $\eta'_{1i}$ ,  $\eta'_{2i}$  and  $\gamma_i$  are the measurement at the knot, mean of two slopes, the half-difference between two slopes and knot for the  $i^{th}$  individual. Through straightforward algebra, the measurement  $y_{ij}$  of the bilinear spline in the right panel, in which the measurement  $y_{ij}$  should always be the maximum value of two lines, has the identical final form as Equation (A.1).

=====  
Insert Figure A.1 about here  
=====

### A.2 Taylor Series Expansion

For the  $i^{th}$  individual, suppose we have a function  $f(\gamma_i)$  and its first derivative with respect to  $\gamma_i$ <sup>8</sup>, shown in equations

$$f(\gamma_i) = \eta'_{0i} + \eta'_{1i}(t_{ij} - \gamma_i) + \eta'_{2i}\sqrt{(t_{ij} - \gamma_i)^2}$$

and

$$f'(\gamma_i) = \eta_{1i} - \eta'_{1i} - \frac{\eta'_{2i}(t_{ij} - \gamma_i)}{\sqrt{(t_{ij} - \gamma_i)^2}} = -\eta'_{2i} - \frac{\eta'_{2i}(t_{ij} - \gamma_i)}{\sqrt{(t_{ij} - \gamma_i)^2}},$$

respectively. Then the Taylor series expansion of  $f(\gamma_i)$  can be expressed as

$$\begin{aligned}
f(\gamma_i) &= f(\mu_\gamma) + \frac{f'(\mu_\gamma)}{1!}(\gamma_i - \mu_\gamma) + \dots \\
&= \eta'_{0i} + \eta'_{1i}(t_{ij} - \mu_\gamma) + \eta'_{2i}\sqrt{(t_{ij} - \mu_\gamma)^2} + (\gamma_i - \mu_\gamma) \left[ -\eta'_{2i} - \frac{\eta'_{2i}(t_{ij} - \mu_\gamma)}{|t_{ij} - \mu_\gamma|} \right] + \dots \\
&\approx \eta'_{0i} + \eta'_{1i}(t_{ij} - \mu_\gamma) + \eta'_{2i}|t_{ij} - \mu_\gamma| + (\gamma_i - \mu_\gamma) \left[ -\mu'_{\eta_2} - \frac{\mu'_{\eta_2}(t_{ij} - \mu_\gamma)}{|t_{ij} - \mu_\gamma|} \right],
\end{aligned}$$

from which we then have the reparameterized growth factors and the corresponding factor loadings for the  $i^{th}$  individual.

<sup>8</sup>It is noted that we have 4 degree-of-freedom when expressing the repeated outcomes of a linear combination of 4 growth factors (Harring et al., 2006). To simplify subsequent calculation, we viewed  $\eta_{0i}$ ,  $\eta_{1i}$ ,  $\eta_{2i}$  and  $\gamma_i$  (i.e., the growth factors in the original setting) as independent variables. It is also noted that  $\gamma_i$  is intact during the process of reparameterization (Preacher and Hancock, 2012).

### A.3 Derivation of transformation matrices and the inverse-transformation matrices between mean vectors and variance-covariance matrices at the population-level

Through straightforward algebra, we can approximate the mean vector of the reparameterized growth factors from the mean vector of their original setting via the following equation

$$\begin{aligned}\boldsymbol{\mu}'_{\eta} &= E(\mathbf{G}_i \times \begin{pmatrix} \eta_{0i} \\ \eta_{1i} \\ \eta_{2i} \\ \gamma_i - \mu_{\gamma} \end{pmatrix}) = E\left[\begin{pmatrix} 1 & \gamma_i & 0 & 0 \\ 0 & 0.5 & 0.5 & 0 \\ 0 & -0.5 & 0.5 & 0 \\ 0 & 0 & 0 & 1 \end{pmatrix} \times \begin{pmatrix} \eta_{0i} \\ \eta_{1i} \\ \eta_{2i} \\ \gamma_i - \mu_{\gamma} \end{pmatrix}\right] \\ &\approx \begin{pmatrix} 1 & \mu_{\gamma} & 0 & 0 \\ 0 & 0.5 & 0.5 & 0 \\ 0 & -0.5 & 0.5 & 0 \\ 0 & 0 & 0 & 1 \end{pmatrix} \times \begin{pmatrix} \mu_{\eta_0} \\ \mu_{\eta_1} \\ \mu_{\eta_2} \\ 0 \end{pmatrix}\end{aligned}$$

under the condition of  $\frac{1}{n} \sum_{i=1}^n Cov(\eta_{1i}, \gamma_i) \rightarrow 0$ .

Similarly, the mean vector of the original parameters can be approximated from the reparameterized setting through the equation

$$\begin{aligned}\boldsymbol{\mu}_{\eta} &= E(\mathbf{G}_i^{-1} \times \begin{pmatrix} \eta'_{0i} \\ \eta'_{1i} \\ \eta'_{2i} \\ \delta_i + \mu_{\gamma} \end{pmatrix}) = E\left[\begin{pmatrix} 1 & -\gamma_i & \gamma_i & 0 \\ 0 & 1 & -1 & 0 \\ 0 & 1 & 1 & 0 \\ 0 & 0 & 0 & 1 \end{pmatrix} \times \begin{pmatrix} \eta'_{0i} \\ \eta'_{1i} \\ \eta'_{2i} \\ \delta_i + \mu_{\gamma} \end{pmatrix}\right] \\ &\approx \begin{pmatrix} 1 & -\mu_{\gamma} & \mu_{\gamma} & 0 \\ 0 & 1 & -1 & 0 \\ 0 & 1 & 1 & 0 \\ 0 & 0 & 0 & 1 \end{pmatrix} \times \begin{pmatrix} \mu'_{\eta_{0i}} \\ \mu'_{\eta_{1i}} \\ \mu'_{\eta_{2i}} \\ \mu_{\gamma} \end{pmatrix}\end{aligned}$$

under the condition of  $\frac{1}{n} \sum_{i=1}^n Cov(\eta_{2i}, \gamma_i) \rightarrow 0$ .

Through variance decomposition, we can approximate the variance-covariance matrix of the reparameterized growth factors from the variance-covariance matrix of their original setting via the following equation

$$\begin{aligned}\boldsymbol{\Psi}'_{\eta} &= Var(\mathbf{G}_i \times \boldsymbol{\eta}_i) = E(Var(\mathbf{G}_i \times \boldsymbol{\eta}_i | \gamma_i)) + Var(E(\mathbf{G}_i \times \boldsymbol{\eta}_i | \gamma_i)) \\ &\approx E(Var(\mathbf{G}_i \times \boldsymbol{\eta}_i | \gamma_i)) = E(\nabla \mathbf{G}_i Var(\boldsymbol{\eta}_i) \nabla \mathbf{G}_i^T) \\ &\approx \begin{pmatrix} 1 & \mu_{\gamma} & 0 & \mu_{\eta_1} \\ 0 & 0.5 & 0.5 & 0 \\ 0 & -0.5 & 0.5 & 0 \\ 0 & 0 & 0 & 1 \end{pmatrix} \boldsymbol{\Psi}_{\eta} \begin{pmatrix} 1 & \mu_{\gamma} & 0 & \mu_{\eta_1} \\ 0 & 0.5 & 0.5 & 0 \\ 0 & -0.5 & 0.5 & 0 \\ 0 & 0 & 0 & 1 \end{pmatrix}^T \\ &= \nabla \mathbf{G} \boldsymbol{\Psi}_{\eta} \nabla \mathbf{G}^T\end{aligned}\tag{A.2}$$

under the condition of  $Var(\gamma_i) \rightarrow 0$  and  $Var(\eta_{1i}) \rightarrow 0$ .

Similarly, the variance-covariance matrix of the original parameters can be approximated from the reparameterized setting through the equation

$$\begin{aligned}\boldsymbol{\Psi}_{\eta} &= Var(\mathbf{G}_i^{-1} \times \boldsymbol{\eta}'_i) = E(Var(\mathbf{G}_i^{-1} \times \boldsymbol{\eta}'_i | \gamma_i)) + Var(E(\mathbf{G}_i^{-1} \times \boldsymbol{\eta}'_i | \gamma_i)) \\ &\approx E(Var(\mathbf{G}_i^{-1} \times \boldsymbol{\eta}'_i | \gamma_i)) = E(\nabla \mathbf{G}_i^{-1} Var(\boldsymbol{\eta}'_i) \nabla \mathbf{G}_i^{-1T}) \\ &\approx \begin{pmatrix} 1 & -\mu_{\gamma} & \mu_{\gamma} & 0 \\ 0 & 1 & -1 & 0 \\ 0 & 1 & 1 & 0 \\ 0 & 0 & 0 & 1 \end{pmatrix} \boldsymbol{\Psi}'_{\eta} \begin{pmatrix} 1 & -\mu_{\gamma} & \mu_{\gamma} & 0 \\ 0 & 1 & -1 & 0 \\ 0 & 1 & 1 & 0 \\ 0 & 0 & 0 & 1 \end{pmatrix}^T \\ &= \nabla \mathbf{G}^{-1} \boldsymbol{\Psi}'_{\eta} \nabla \mathbf{G}^{-1T}.\end{aligned}\tag{A.3}$$

under the condition of  $Var(\gamma_i) \rightarrow 0$ .

Through the above equations, we noticed that the most critical condition for the approximation to the population-level transformation is  $Var(\gamma_i) \rightarrow 0$ . With this condition, the covariances of the knot with other growth factors approach to 0. More importantly, the second item of the expression of variance decomposition in Equations (A.2) and (A.3) approaches to 0 given  $Var(\gamma_i) \rightarrow 0$ . Though Equation (A.2) requires  $Var(\eta_{1i}) \rightarrow 0$ , whether to satisfy this condition or not does not affect estimation process.

#### A.4 Details of the transformation matrices and the inverse-transformation matrices between intercept coefficients and path coefficients

$$\begin{aligned}
\mu'_\eta &\approx \mathbf{G} \times \mu_\eta \iff E(\alpha' + \mathbf{B}' \mathbf{X}_i) \approx \mathbf{G} \times E(\alpha + \mathbf{B} \mathbf{X}_i) \iff \alpha' \approx \mathbf{G} \times \alpha \\
\mu_\eta &\approx \mathbf{G}^{-1} \times \mu'_\eta \iff E(\alpha + \mathbf{B} \mathbf{X}_i) \approx \mathbf{G}^{-1} \times E(\alpha' + \mathbf{B}' \mathbf{X}_i) \iff \alpha \approx \mathbf{G}^{-1} \times \alpha' \\
\Psi'_\eta &\approx \nabla \mathbf{G} \Psi_\eta \nabla \mathbf{G}^T \\
&\iff \text{Var}(\alpha' + \mathbf{B}' \mathbf{X}_i + \zeta'_i) \approx \nabla \mathbf{G} \text{Var}(\alpha + \mathbf{B} \mathbf{X}_i + \zeta_i) \nabla \mathbf{G}^T \\
&\iff \text{Var}(\mathbf{B}' \mathbf{X}_i + \zeta'_i) \approx \nabla \mathbf{G} \text{Var}(\mathbf{B} \mathbf{X}_i + \zeta_i) \nabla \mathbf{G}^T \\
&\iff \mathbf{B}' \text{Var}(\mathbf{X}_i) \mathbf{B}^T + \text{Var}(\zeta'_i) \approx \nabla \mathbf{G} \mathbf{B} \text{Var}(\mathbf{X}_i) \mathbf{B}^T \nabla \mathbf{G}^T + \nabla \mathbf{G} \text{Var}(\zeta_i) \nabla \mathbf{G}^T \\
&\iff \mathbf{B}' \approx \nabla \mathbf{G} \mathbf{B} \\
\Psi_\eta &\approx \nabla \mathbf{G}^{-1} \Psi'_\eta \nabla \mathbf{G}^{-1T} \\
&\iff \text{Var}(\alpha + \mathbf{B} \mathbf{X}_i + \zeta_i) \approx \nabla \mathbf{G}^{-1} \text{Var}(\alpha' + \mathbf{B}' \mathbf{X}_i + \zeta'_i) \nabla \mathbf{G}^{-1T} \\
&\iff \text{Var}(\mathbf{B} \mathbf{X}_i + \zeta_i) \approx \nabla \mathbf{G}^{-1} \text{Var}(\mathbf{B}' \mathbf{X}_i + \zeta'_i) \nabla \mathbf{G}^{-1T} \\
&\iff \mathbf{B} \text{Var}(\mathbf{X}_i) \mathbf{B}^T + \text{Var}(\zeta_i) \approx \nabla \mathbf{G}^{-1} \mathbf{B}' \text{Var}(\mathbf{X}_i) \mathbf{B}'^T \nabla \mathbf{G}^{-1T} + \nabla \mathbf{G}^{-1} \text{Var}(\zeta'_i) \nabla \mathbf{G}^{-1T} \\
&\iff \mathbf{B} \approx \nabla \mathbf{G}^{-1} \mathbf{B}'
\end{aligned}$$

#### A.5 Expression of each cell of the re-reparameterized mean vector and variance-covariance matrix

$$\begin{aligned}
\mu_{\eta_0} &\approx \mu'_{\eta_0} - \mu_\gamma \mu'_{\eta_1} + \mu_\gamma \mu'_{\eta_2} \\
\mu_{\eta_1} &= \mu'_{\eta_1} - \mu'_{\eta_2} \\
\mu_{\eta_2} &= \mu'_{\eta_2} + \mu'_{\eta_1} \\
\mu_\gamma &= \mu_\gamma \\
\psi_{00} &\approx (\psi'_{11} + \psi'_{22} - 2\psi'_{12})\mu_\gamma^2 + 2(\psi'_{02} - \psi'_{01})\mu_\gamma + \psi'_{00} \\
\psi_{01} &\approx (2\psi'_{12} - \psi'_{11} - \psi'_{22})\mu_\gamma + (\psi'_{01} - \psi'_{02}) \\
\psi_{02} &\approx (\psi'_{22} - \psi'_{11})\mu_\gamma + (\psi'_{01} + \psi'_{02}) \\
\psi_{0\gamma} &\approx (\psi'_{2\gamma} - \psi'_{1\gamma})\mu_\gamma + \psi'_{0\gamma} \\
\psi_{11} &= \psi'_{11} + \psi'_{22} - 2\psi'_{12} \\
\psi_{12} &= \psi'_{11} - \psi'_{22} \\
\psi_{1\gamma} &= \psi'_{1\gamma} - \psi'_{2\gamma} \\
\psi_{22} &= \psi'_{11} + \psi'_{22} + 2\psi'_{12} \\
\psi_{2\gamma} &= \psi'_{1\gamma} + \psi'_{2\gamma} \\
\psi_{\gamma\gamma} &= \psi'_{\gamma\gamma}
\end{aligned}$$

#### A.6 Generate Exogenous Variables and Growth Factors Simultaneously

To generate growth factors and exogenous variables simultaneously as a multivariate normal distribution, we need to specify the mean vector and the variance-covariance matrix of the distribution. In our setting, the mean vector can be represented in equation

$$\boldsymbol{\mu} = (\boldsymbol{\alpha} \quad 0 \quad 0),$$

where  $\boldsymbol{\alpha}$  and  $(0 \quad 0)$  are the mean vector of the growth factors and that of the TICs, respectively. Moreover, through straightforward linear algebra, the underlying variance-covariance matrix of the distribution is

$$\boldsymbol{\Sigma} = \begin{pmatrix} \mathbf{B}\boldsymbol{\Phi}\mathbf{B} + \boldsymbol{\Psi}_\eta & \mathbf{B}\boldsymbol{\Phi} \\ \mathbf{B}\boldsymbol{\Phi} & \boldsymbol{\Phi} \end{pmatrix},$$

where  $\mathbf{B}$  is the matrix of path coefficients,  $\Psi_{\eta}$  and  $\Phi$  are the variance-covariance matrices of the growth factors and the TICs, respectively. Accordingly, we can generate the growth factors and TICs simultaneously, which follows a multivariate normal distribution  $N_6(\boldsymbol{\mu}, \boldsymbol{\Sigma})$ .

## References

- Bauer, D. J. and Curran, P. J. (2003). Distributional assumptions of growth mixture models: Implications for overextraction of latent trajectory classes. *Psychological Methods*, 8(3):338–363.
- Boker, S. M., Neale, M. C., Maes, H. H., Wilde, M. J., Spiegel, M., Brick, T. R., Estabrook, R., Bates, T. C., Mehta, P., von Oertzen, T., Gore, R. J., Hunter, M. D., Hackett, D. C., Karch, J., Brandmaier, A. M., Pritikin, J. N., Zahery, M., Kirkpatrick, R. M., Wang, Y., Driver, C., Massachusetts Institute of Technology, Johnson, S. G., Association for Computing Machinery, Kraft, D., Wilhelm, S., and Manjunath, B. G. (2018). *OpenMx 2.9.6 User Guide*.
- Bollen, K. A. and Curran, P. J. (2005). *Nonlinear Trajectories and the Coding of Time*, chapter 4, pages 88–125. John Wiley & Sons, Inc.
- Browne, M. W. and du Toit, S. H. C. (1991). Models for learning data. In Collins, L. M. and Horn, J. L., editors, *Best methods for the analysis of change: Recent advances, unanswered questions, future directions*, chapter 4, pages 47–68. American Psychological Association., Washington, DC, US.
- Chou, C.-P., Yang, D., Pentz, M. A., and Hser, Y. I. (2004). Piecewise growth curve modeling approach for longitudinal prevention study. *Computational Statistics & Data Analysis*, 46(2):213–225.
- Cohen, J. (1988). *Multiple Regression and Correlation Analysis*, chapter 9, pages 407–466. Lawrence Erlbaum Associates.
- Cook, N. R. and Ware, J. H. (1983). Design and analysis methods for longitudinal research. *Annual Review of Public Health*, 4(1):1–23.
- Coulombe, P., Selig, J. P., and Delaney, H. D. (2015). Ignoring individual differences in times of assessment in growth curve modeling. *International Journal of Behavioral Development*, 40(1):76–86.
- Cudeck, R. and du Toit, S. H. C. (2003). Nonlinear multilevel models for repeated measures data. In Reise, S. P. and Duan, N., editors, *Multilevel Modeling: Methodological Advances, Issues, and Applications*., Multivariate Applications Book Series, chapter 2, pages 1–24. Psychology Press.
- Cudeck, R. and Harring, J. R. (2010). Developing a random coefficient model for nonlinear repeated measures data. In Chow, S.-M., Ferrer, E., and Hsieh, F., editors, *The Notre Dame series on quantitative methodology. Statistical methods for modeling human dynamics: An interdisciplinary dialogue*, chapter 2, pages 289–318. Routledge/Taylor & Francis Group., New York, NY: Routledge.
- Cudeck, R. and Klebe, K. J. (2002). Multiphase mixed-effects models for repeated measures data. *Psychological Methods*, 7(1):41–63.
- Dominicus, A., Ripatti, S., Pedersen, N. L., and Palmgren, J. (2008). A random change point model for assessing variability in repeated measures of cognitive function. *Statistics in Medicine*, 27(27):5786–5798.
- Dumenci, L., Perera, R. A., Keefe, F. J., Ang, D. C., J., S., Jensen, M. P., and Riddle, D. L. (2019). Model-based pain and function outcome trajectory types for patients undergoing knee arthroplasty: a secondary analysis from a randomized clinical trial. *Osteoarthritis and cartilage*, 27(6):878–884.
- Finkel, D., Reynolds, C., Mcardle, J., Gatz, M., and L Pedersen, N. (2003). Latent growth curve analyses of accelerating decline in cognitive abilities in late adulthood. *Developmental psychology*, 39:535–550.
- Flora, D. B. (2008). Specifying piecewise latent trajectory models for longitudinal data. *Structural Equation Modeling: A Multidisciplinary Journal*, 15(3):513–533.
- Grimm, K. J., Ram, N., and Estabrook, R. (2016a). *Growth Models with Nonlinearity in Parameters*, chapter 11, pages 234–274. Guilford Press.
- Grimm, K. J., Ram, N., and Estabrook, R. (2016b). *Growth Models with Nonlinearity in Random Coefficients*, chapter 12, pages 275–308. Guilford Press.
- Harring, J. R., Cudeck, R., and du Toit, S. H. C. (2006). Fitting partially nonlinear random coefficient models as sems. *Multivariate Behavioral Research*, 41(4):579–596.
- Hedeker, D., Mermelstein, R. J., and Flay, B. R. (2006). Application of item response theory models for intensive longitudinal data. In Walls, T. A. and Schafer, J. L., editors, *Models for Intensive Longitudinal Data*, chapter 4, pages 84–108. Oxford University Press, ProQuest Ebook Central.

- Hunter, M. D. (2018). State space modeling in an open source, modular, structural equation modeling environment. *Structural Equation Modeling*, 25(2):307–324.
- Kohli, N. (2011). *Estimating unknown knots in piecewise linear-linear latent growth mixture models*. PhD thesis, University of Maryland.
- Kohli, N. and Harring, J. R. (2013). Modeling growth in latent variables using a piecewise function. *Multivariate Behavioral Research*, 48(3):370–397.
- Kohli, N., Harring, J. R., and Hancock, G. R. (2013). Piecewise linear-linear latent growth mixture models with unknown knots. *Educational and Psychological Measurement*, 73(6):935–955.
- Kohli, N., Hughes, J., Wang, C., Zopluoglu, C., and Davison, M. L. (2015a). Fitting a linear-linear piecewise growth mixture model with unknown knots: A comparison of two common approaches to inference. *Psychological Methods*, 20(2):259–275.
- Kohli, N., Sullivan, A. L., Sadeh, S., and Zopluoglu, C. (2015b). Longitudinal mathematics development of students with learning disabilities and students without disabilities: A comparison of linear, quadratic, and piecewise linear mixed effects models. *Journal of School Psychology*, 53(2):105–120.
- Kwok, O., Luo, W., and West, S. G. (2010). Using modification indexes to detect turning points in longitudinal data: A monte carlo study. *Structural Equation Modeling: A Multidisciplinary Journal*, 17(2):216–240.
- Lê, T., Norman, G., Tourangeau, K., Brick, J. M., and Mulligan, G. (2011). Early childhood longitudinal study: Kindergarten class of 2010-2011 – sample design issues. *JSM Proceedings*, pages 1629–1639.
- Li, F., Duncan, T. E., Duncan, S. C., and Hops, H. (2001). Piecewise growth mixture modeling of adolescent alcohol use data. *Structural Equation Modeling: A Multidisciplinary Journal*, 8(2):175–204.
- Liu, J. (2019). *Estimating Knots in Bilinear Spline Growth Models with Time-invariant Covariates in the Framework of Individual Measurement Occasions*. PhD thesis, Virginia Commonwealth University.
- Lock, E. F., Kohli, N., and Bose, M. (2018). Detecting multiple random changepoints in bayesian piecewise growth mixture models. *Psychometrika*, 83(3):733–750.
- Marcoulides, K. M. (2018). Automated latent growth curve model fitting: A segmentation and knot selection approach. *Structural Equation Modeling: A Multidisciplinary Journal*, 25(5):687–699.
- McArdle, J. J. and Wang, L. (2008). Modeling age-based turning points in longitudinal life-span growth curves of cognition. In Cohen, P., editor, *Applied data analytic techniques for turning points research*, Multivariate applications series., chapter 2, pages 1–24. Routledge/Taylor & Francis Group.
- Mehta, P. D. and Neale, M. C. (2005). People are variables too: Multilevel structural equations modeling. *Psychological Methods*, 10(3):259–284.
- Mehta, P. D. and West, S. G. (2000). Putting the individual back into individual growth curves. *Psychological Methods*, 5(1):23–43.
- Morris, T. P., White, I. R., and Crowther, M. J. (2019). Using simulation studies to evaluate statistical methods. *Statistics in Medicine*, 38(11):2074–2102.
- Muniz Terrera, G., van den Hout, A., and Matthews, F. E. (2011). Random change point models: investigating cognitive decline in the presence of missing data. *Journal of Applied Statistics.*, 38(4):705–716.
- Neale, M. C., Hunter, M. D., Pritikin, J. N., Zahery, M., Brick, T. R., Kirkpatrick, R. M., Estabrook, R., Bates, T. C., Maes, H. H., and Boker, S. M. (2016). OpenMx 2.0: Extended structural equation and statistical modeling. *Psychometrika*, 81(2):535–549.
- Preacher, K. J. and Hancock, G. R. (2012). On interpretable reparameterizations of linear and nonlinear latent growth curve models. In Harring, J. R. and Hancock, G. R., editors, *CILVR series on latent variable methodology. Advances in longitudinal methods in the social and behavioral sciences*, chapter 2, pages 25–58. IAP Information Age Publishing, Charlotte, NC, US.
- Preacher, K. J. and Hancock, G. R. (2015). Meaningful aspects of change as novel random coefficients: A general method for reparameterizing longitudinal models. *Psychological Methods*, 20(1):84–101.
- Pritikin, J. N., Hunter, M. D., and Boker, S. M. (2015). Modular open-source software for Item Factor Analysis. *Educational and Psychological Measurement*, 75(3):458–474.
- Riddle, D. L., Perera, R. A., Jiranek, W. A., and Dumenci, L. (2015). Using surgical appropriateness criteria to examine outcomes of total knee arthroplasty in a united states sample. *Arthritis care & research.*, 67(3):349–357.
- Seber, G. A. F. and Wild, C. J. (2003). *Nonlinear Regression*. John Wiley & Sons, Inc.

- Sterba, S. K. (2014). Fitting nonlinear latent growth curve models with individually varying time points. *Structural Equation Modeling: A Multidisciplinary Journal*, 21(4):630–647.
- Sullivan, A. L., Kohli, N., Farnsworth, E. M., Sadeh, S., and Jones, L. (2017). Longitudinal models of reading achievement of students with learning disabilities and without disabilities. *School psychology quarterly: the official journal of the Division of School Psychology, American Psychological Association*, 32(3):336–349.
- Tishler, A. and Zang, I. (1981). A maximum likelihood method for piecewise regression models with a continuous dependent variable. *Journal of the Royal Statistical Society. Series C. Applied Statistics*, 30.
- Venables, W. N. and Ripley, B. D. (2002). *Modern Applied Statistics with S*. Springer, New York, fourth edition.
- Wang, L. and McArdle, J. J. (2008). A simulation study comparison of bayesian estimation with conventional methods for estimating unknown change points. *Structural Equation Modeling: A Multidisciplinary Journal*, 15(1):52–74.

Table 1: Performance Metric: Definitions and Estimates

Criteria	Definition	Estimate
Relative Bias	$E_{\hat{\theta}}(\hat{\theta} - \theta)/\theta$	$\sum_{s=1}^S (\hat{\theta}_s - \theta)/S\theta$
Empirical SE	$\sqrt{Var(\hat{\theta})}$	$\sqrt{\sum_{s=1}^S (\hat{\theta}_s - \bar{\theta})^2 / (S - 1)}$
Relative RMSE	$\sqrt{E_{\hat{\theta}}(\hat{\theta} - \theta)^2 / \theta}$	$\sqrt{\sum_{s=1}^S (\hat{\theta}_s - \theta)^2 / S / \theta}$
Coverage Probability	$Pr(\hat{\theta}_{low} \leq \theta \leq \hat{\theta}_{upper})$	$\sum_{s=1}^S I(\hat{\theta}_{low,s} \leq \theta \leq \hat{\theta}_{upper,s})$

<sup>1</sup>  $\theta$ : the population value of the parameter of interest

<sup>2</sup>  $\hat{\theta}$ : the estimate of  $\theta$

<sup>3</sup>  $S$ : the number of replications and set as 1,000 in our simulation study

<sup>4</sup>  $s = 1, \dots, S$ : indexes the replications of the simulation

<sup>5</sup>  $\hat{\theta}_s$ : the estimate of  $\theta$  from the  $s^{th}$  replication

<sup>6</sup>  $\bar{\theta}$ : the mean of  $\hat{\theta}_s$ 's across replications

<sup>7</sup>  $I()$ : an indicator function

Table 2: Simulation Design for the Models

Fixed Conditions	
Variables	Conditions
Mean of the Intercept	$\mu_{\eta_0} = 100$
Variance of the Intercept	$\psi_{00} = 25$
Mean of the 1st Slope	$\mu_{\eta_1} = -5$
Variance of Slopes	$\psi_{11} = \psi_{22} = 1$
Correlations of Growth Factors	$\rho = 0.3$
Manipulated Conditions	
Partially Crossed Design	
Variables	Conditions
Time ( $t_j$ )	6 scaled and equally spaced ( $j = 0 \dots, J - 1, J = 6$ ) 10 scaled and equally spaced ( $j = 0, \dots, J - 1, J = 10$ )
(Mean of) the knot	$\mu_{\gamma}$ at $t = 2.5$ for $J = 6$ $\mu_{\gamma}$ at $t = 3.5$ or $4.5$ or $5.5$ for $J = 10$
Individual $t_{ij}$	$t_{ij} \sim U(t_j - \Delta, t_j + \Delta) (j = 0, \dots, J - 1; \Delta = 0.25)$
Sample Size	$n = 200$ $n = 500$
Full Factorial Design	
Variables	Conditions
Standardized Difference $d_z$	$\mu_{\eta_1} - \mu_{\eta_2} = \pm 1.6$ (1.0-unit Standardized Difference) $\mu_{\eta_1} - \mu_{\eta_2} = \pm 2.4$ (1.5-unit Standardized Difference) $\mu_{\eta_1} - \mu_{\eta_2} = \pm 3.2$ (2.0-unit Standardized Difference)
Variance of Knots	$\psi_{\gamma\gamma} = 0$ ( $sd(\gamma)/(t_j - t_{j-1}) = 0$ ) $\psi_{\gamma\gamma} = 0.09$ ( $sd(\gamma)/(t_j - t_{j-1}) = 0.3$ ) $\psi_{\gamma\gamma} = 0.36$ ( $sd(\gamma)/(t_j - t_{j-1}) = 0.6$ )
Coefficients ( $B$ )	TICs explain 13% variability of growth factors TICs explain 26% variability of growth factors
Residual Variance	$\theta_{\epsilon} = 1$ $\theta_{\epsilon} = 2$

Table 3: Number of Improper Solutions among 1,000 Convergent Replications under Conditions with 10 Repeated Measures & Midway Knot, 13% Explained Variance

		$\theta_\epsilon = 1$		$\theta_\epsilon = 2$		
		$n = 200$	$n = 500$	$n = 200$	$n = 500$	
Small $d_z$	Positive $d_z$	$sd(\gamma) = 0$	555//48 <sup>1</sup>	516//22	550//40	507//29
		$sd(\gamma) = 0.3$	117//35	7//11	278//48	168//21
		$sd(\gamma) = 0.6$	4//3	0//0	58//25	7//6
	Negative $d_z$	$sd(\gamma) = 0$	535//37	542//27	568//44	531//27
		$sd(\gamma) = 0.3$	106//49	24//14	279//59	134//39
		$sd(\gamma) = 0.6$	0//8	0//0	67//45	8//17
Medium $d_z$	Positive $d_z$	$sd(\gamma) = 0$	563//49	553//28	583//39	573//22
		$sd(\gamma) = 0.3$	17//14	1//0	141//27	40//11
		$sd(\gamma) = 0.6$	0//1	0//0	9//2	0//0
	Negative $d_z$	$sd(\gamma) = 0$	568//42	542//26	576//50	513//32
		$sd(\gamma) = 0.3$	19//17	1//0	130//64	22//32
		$sd(\gamma) = 0.6$	0//0	0//0	4//23	0//0
Large $d_z$	Positive $d_z$	$sd(\gamma) = 0$	555//44	555//36	562//45	557//19
		$sd(\gamma) = 0.3$	1//0	0//0	27//19	0//0
		$sd(\gamma) = 0.6$	0//0	0//0	0//0	0//0
	Negative $d_z$	$sd(\gamma) = 0$	548//35	514//30	555//36	523//33
		$sd(\gamma) = 0.3$	1//2	0//0	37//39	2//6
		$sd(\gamma) = 0.6$	0//0	0//0	0//2	0//0

<sup>1</sup> 555//48 indicates that among 1,000 convergent replications, we have 555 and 48 improper solutions due to negative knot variances and out-of-range correlations of the knot with other growth factors, respectively.

Table 4: Median (Range) of Relative Bias of Each Parameter Across Conditions with 10 Repeated Measures & Midway Knot

	Para.	Reduced Model	Full Model
		Median (Range)	Median (Range)
<b>Mean Vector</b>	$\mu_{\eta_0}$	0.0000 (-0.0005, 0.0006)	0.0000 (-0.0006, 0.0006)
	$\mu_{\eta_1}$	0.0000 (-0.0098, 0.0100)	0.0000 (-0.0099, 0.0100)
	$\mu_{\eta_2}$	0.0000 (-0.0063, 0.0280)	0.0000 (-0.0062, 0.0273)
	$\mu_\gamma$	0.0000 (-0.0014, 0.0009)	0.0000 (-0.0017, 0.0006)
<b>Path Coef. of <math>x_1</math></b>	$\beta_{10}$	0.0030 (-0.0823, 0.0773)	0.0027 (-0.0345, 0.0367)
	$\beta_{11}$	0.0023 (-0.3069, 0.3055)	0.0010 (-0.1113, 0.1052)
	$\beta_{12}$	0.0016 (-0.2984, 0.2970)	0.0002 (-0.0940, 0.0946)
	$\beta_{1\gamma}$	— <sup>1</sup>	-0.2712 (NA, <sup>2</sup> NA)
	$\beta_{20}$	0.0006 (-0.0697, 0.0690)	0.0007 (-0.0216, 0.0250)
<b>Path Coef. of <math>x_2</math></b>	$\beta_{21}$	0.0006 (-0.2901, 0.2950)	0.0000 (-0.0882, 0.0933)
	$\beta_{22}$	-0.0017 (-0.2888, 0.2901)	-0.0019 (-0.0901, 0.0878)
	$\beta_{2\gamma}$	—	-0.2709 (NA, NA)
	$\psi_{00}$	-0.0107 (-0.0409, 0.0212)	-0.0107 (-0.0235, 0.0018)
<b>Unexplained Variance</b>	$\psi_{11}$	-0.0070 (-0.0753, 0.1692)	-0.0138 (-0.0657, 0.0182)
	$\psi_{22}$	-0.0080 (-0.0703, 0.1638)	-0.0130 (-0.0647, 0.0132)
	$\psi_{\gamma\gamma}$	—	0.0403 (-0.4151, NA)

<sup>1</sup> — indicates that the relative biases are not available from the reduced model.

<sup>2</sup> NA indicates that the bounds of relative bias is not available. The model performance under the conditions with 0 population value of difference in knot is of interest where the relative bias of those knot coefficients would go infinity.

Table 5: Median (Range) of Empirical Standard Error of Each Parameter Across Conditions with 10 Repeated Measures &amp; Midway Knot

	Para.	Reduced Model	Full Model
		Median (Range)	Median (Range)
<b>Mean Vector</b>	$\mu_{\eta_0}$	0.2576 (0.1903, 0.3550)	0.2578 (0.1903, 0.3547)
	$\mu_{\eta_1}$	0.0548 (0.0387, 0.0755)	0.0548 (0.0387, 0.0755)
	$\mu_{\eta_2}$	0.0552 (0.0400, 0.0755)	0.0552 (0.0400, 0.0762)
	$\mu_{\gamma}$	0.0418 (0.0173, 0.0854)	0.0412 (0.0173, 0.0922)
<b>Path Coef. of <math>x_1</math></b>	$\beta_{10}$	0.2761 (0.1957, 0.3734)	0.2768 (0.1967, 0.3735)
	$\beta_{11}$	0.0579 (0.0412, 0.0800)	0.0583 (0.0412, 0.0806)
	$\beta_{12}$	0.0574 (0.0412, 0.0819)	0.0583 (0.0412, 0.0819)
	$\beta_{1\gamma}$	— <sup>1</sup>	0.0387 (0.0100, 0.0990)
<b>Path Coef. of <math>x_2</math></b>	$\beta_{20}$	0.2725 (0.1980, 0.3744)	0.2720 (0.1980, 0.3751)
	$\beta_{21}$	0.0574 (0.0412, 0.0806)	0.0583 (0.0412, 0.0806)
	$\beta_{22}$	0.0578 (0.0412, 0.0800)	0.0582 (0.0412, 0.0812)
	$\beta_{2\gamma}$	—	0.0400 (0.0100, 0.1054)
<b>Unexplained Variance</b>	$\psi_{00}$	1.6912 (1.1734, 2.3690)	1.6902 (1.1741, 2.3501)
	$\psi_{11}$	0.0748 (0.0490, 0.1122)	0.0747 (0.0490, 0.1095)
	$\psi_{22}$	0.0741 (0.0490, 0.1140)	0.0740 (0.0510, 0.1091)
	$\psi_{\gamma\gamma}$	—	0.0387 (0.0000, 0.1732)

<sup>1</sup> — indicates that the empirical standard errors are not available from the reduced model.

Table 6: Median (Range) of Relative RMSE of Each Parameter Across Conditions with 10 Repeated Measures &amp; Midway Knot

	Para.	Reduced Model	Full Model
		Median (Range)	Median (Range)
<b>Mean Vector</b>	$\mu_{\eta_0}$	0.0026 (0.0019, 0.0035)	0.0026 (0.0019, 0.0035)
	$\mu_{\eta_1}$	-0.0128 (-0.0178, -0.0078)	-0.0128 (-0.0178, -0.0078)
	$\mu_{\eta_2}$	-0.0118 (-0.0498, -0.0050)	-0.0120 (-0.0490, -0.0050)
	$\mu_{\gamma}$	0.0092 (0.0036, 0.0190)	0.0092 (0.0037, 0.0204)
<b>Path Coef. of <math>x_1</math></b>	$\beta_{10}$	0.2594 (0.1595, 0.4266)	0.2568 (0.1570, 0.4227)
	$\beta_{11}$	0.2980 (0.1656, 0.5418)	0.2752 (0.1678, 0.4674)
	$\beta_{12}$	0.2912 (0.1634, 0.5378)	0.2734 (0.1646, 0.4641)
	$\beta_{1\gamma}$	— <sup>1</sup>	0.7689 (0.3162, NA) <sup>2</sup>
<b>Path Coef. of <math>x_2</math></b>	$\beta_{20}$	0.1747 (0.1063, 0.2865)	0.1722 (0.1059, 0.2830)
	$\beta_{21}$	0.2234 (0.1104, 0.4097)	0.1860 (0.1114, 0.3068)
	$\beta_{22}$	0.2234 (0.1091, 0.4122)	0.1834 (0.1104, 0.3061)
	$\beta_{2\gamma}$	—	0.5625 (0.2179, NA)
<b>Unexplained Variance</b>	$\psi_{00}$	0.0856 (0.0610, 0.1111)	0.0846 (0.0610, 0.1112)
	$\psi_{11}$	0.1076 (0.0655, 0.1998)	0.0982 (0.0664, 0.1360)
	$\psi_{22}$	0.1078 (0.0663, 0.2038)	0.0988 (0.0666, 0.1326)
	$\psi_{\gamma\gamma}$	—	0.6089 (0.2130, NA)

<sup>1</sup> — indicates that the relative RMSEs are not available from the reduced model.

<sup>2</sup> NA indicates that the upper bound of relative RMSE is not available. The model performance under the conditions with 0 population value of difference in knot is of interest where the relative RMSE of those knot coefficients would go infinity.

Table 7: Median (Range) of Coverage Probability of Each Parameter Across Conditions with 10 Repeated Measures & Midway Knot

	<b>Para.</b>	<b>Reduced Model</b> Median (Range)	<b>Full Model</b> Median (Range)
<b>Mean Vector</b>	$\mu_{\eta_0}$	0.9470 (0.9280, 0.9680)	0.9459 (0.9203, 0.9677) <sup>1</sup>
	$\mu_{\eta_1}$	0.9430 (0.7800, 0.9660)	0.9418 (0.7660, 0.9744)
	$\mu_{\eta_2}$	0.9440 (0.7970, 0.9670)	0.9429 (0.7990, 0.9702)
	$\mu_{\gamma}$	0.9100 (0.7880, 0.9680)	0.9510 (0.9267, 0.9758)
<b>Path Coef. of <math>x_1</math></b>	$\beta_{10}$	0.9460 (0.9140, 0.9620)	0.9472 (0.8926, 0.9745)
	$\beta_{11}$	0.9295 (0.6170, 0.9630)	0.9450 (0.9070, 0.9673)
	$\beta_{12}$	0.9290 (0.6120, 0.9630)	0.9460 (0.9080, 0.9823)
	$\beta_{1\gamma}$	— <sup>2</sup>	0.9463 (0.6640, 0.9751)
<b>Path Coef. of <math>x_2</math></b>	$\beta_{20}$	0.9440 (0.8950, 0.9590)	0.9479 (0.9220, 0.9685)
	$\beta_{21}$	0.9090 (0.2780, 0.964)	0.9440 (0.8820, 0.9745)
	$\beta_{22}$	0.9130 (0.2960, 0.9650)	0.9445 (0.8720, 0.9703)
	$\beta_{2\gamma}$	—	0.9416 (0.3810, 0.9879)
<b>Unexplained Variance</b>	$\psi_{00}$	0.9375 (0.8970, 0.9600)	0.9389 (0.9086, 0.9627)
	$\psi_{11}$	0.9365 (0.4240, 0.9600)	0.9351 (0.8550, 0.9728)
	$\psi_{22}$	0.9370 (0.4660, 0.9620)	0.9360 (0.8570, 0.9698)
	$\psi_{\gamma\gamma}$	—	0.9620 (0.0030, 0.9976)

<sup>1</sup> For the full model, the reported coverage probabilities have four decimals since we calculated the coverage probabilities only based on the replications with proper solutions.

<sup>2</sup> — indicates that the coverage probabilities are not available from the reduced model.

Table 8: Summary of Model Fit Information For the Models

<b>Latent Growth Curve Models</b>					
<b>Model</b>	<b>-2loglikelihood</b>	<b>AIC</b>	<b>BIC</b>	<b># of Para.</b>	<b>Residual</b>
Linear	27298	27310	27334	6	75.60
Quadratic	25320	25340	25379	10	35.14
Jenss-Bayley	25330	25352	25396	11	35.37
Linear-linear Piecewise w/ a Fixed Knot	25412	25434	25477	11	36.84
Linear-linear Piecewise w/ a Random Knot	25308	25338	25398	15	33.06
<b>Latent Growth Curve Models with TICs (Time Structure: Age in Months)</b>					
<b>Model</b>	<b>-2loglikelihood</b>	<b>AIC</b>	<b>BIC</b>	<b># of Para.</b>	<b>Residual</b>
Proposed Model	31677	31809	32073	66	33.00
<b>Latent Growth Curve Models with TICs (Time Structure: Grade in Months)</b>					
<b>Model</b>	<b>-2loglikelihood</b>	<b>AIC</b>	<b>BIC</b>	<b># of Para.</b>	<b>Residual</b>
Proposed Model	31675	31807	32070	66	34.30

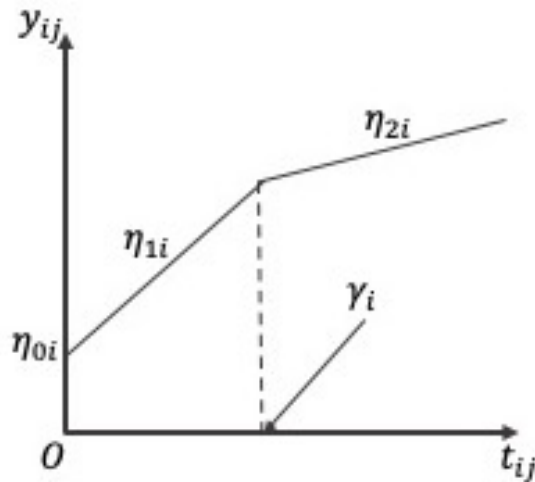


Figure 1: Within-individual Change over Time with Bilinear Spline Functional Form

Table 9: Estimates of the Parameters of Mathematics Trajectories

<b>Growth Factor</b> <b>Parameter</b>	<b>Intercept</b>			<b>First Slope</b>		
	<b>Estimate</b>	<b>SE</b>	<b>P value</b>	<b>Estimate</b>	<b>SE</b>	<b>P value</b>
<b>Mean</b>	26.859	0.588	< 0.0001*	1.731	0.018	< 0.0001*
<b>Unexplained Variance</b>	106.223	9.805	< 0.0001*	0.082	0.010	< 0.0001*
<b>Sex</b> (0–Boy; 1–Girl)	0.349	0.591	0.5548	–0.040	0.019	0.0353*
<b>Race</b> (0–White; 1–Other)	–0.432	0.597	0.4693	0.032	0.019	0.0921
<b>School Location</b>	–0.578	0.609	0.3426	–0.023	0.019	0.2261
<b>Income</b>	1.784	0.801	0.0259*	0.057	0.025	0.0226*
<b>School Type</b> (0–Public; 1–Private)	1.875	0.605	0.0019*	–0.028	0.019	0.1406
<b>Parents’ Highest Education</b>	2.870	0.782	0.0002*	0.046	0.024	0.0553
<b>Growth Factor</b> <b>Parameter</b>	<b>Second Slope</b>			<b>Knot</b>		
	<b>Estimate</b>	<b>SE</b>	<b>P value</b>	<b>Estimate</b>	<b>SE</b>	<b>P value</b>
<b>Mean</b>	0.689	0.017	< 0.0001*	101.737	0.523	< 0.0001*
<b>Unexplained Variance</b>	0.014	0.008	0.0801	42.537	8.086	< 0.0001*
<b>Sex</b> (0–Boy; 1–Girl)	0.020	0.017	0.2394	–0.828	0.523	0.1134
<b>Race</b> (0–White; 1–Other)	–0.028	0.017	0.0995	–0.248	0.536	0.6436
<b>School Location</b>	–0.016	0.017	0.3466	1.612	0.539	0.0028*
<b>Income</b>	0.019	0.023	0.4088	–0.606	0.676	0.3700
<b>School Type</b> (0–Public; 1–Private)	–0.026	0.018	0.1486	0.114	0.529	0.8294
<b>Parents’ Highest Education</b>	–0.023	0.022	0.2958	0.300	0.658	0.6484

\* indicates statistical significance at 0.05 level.

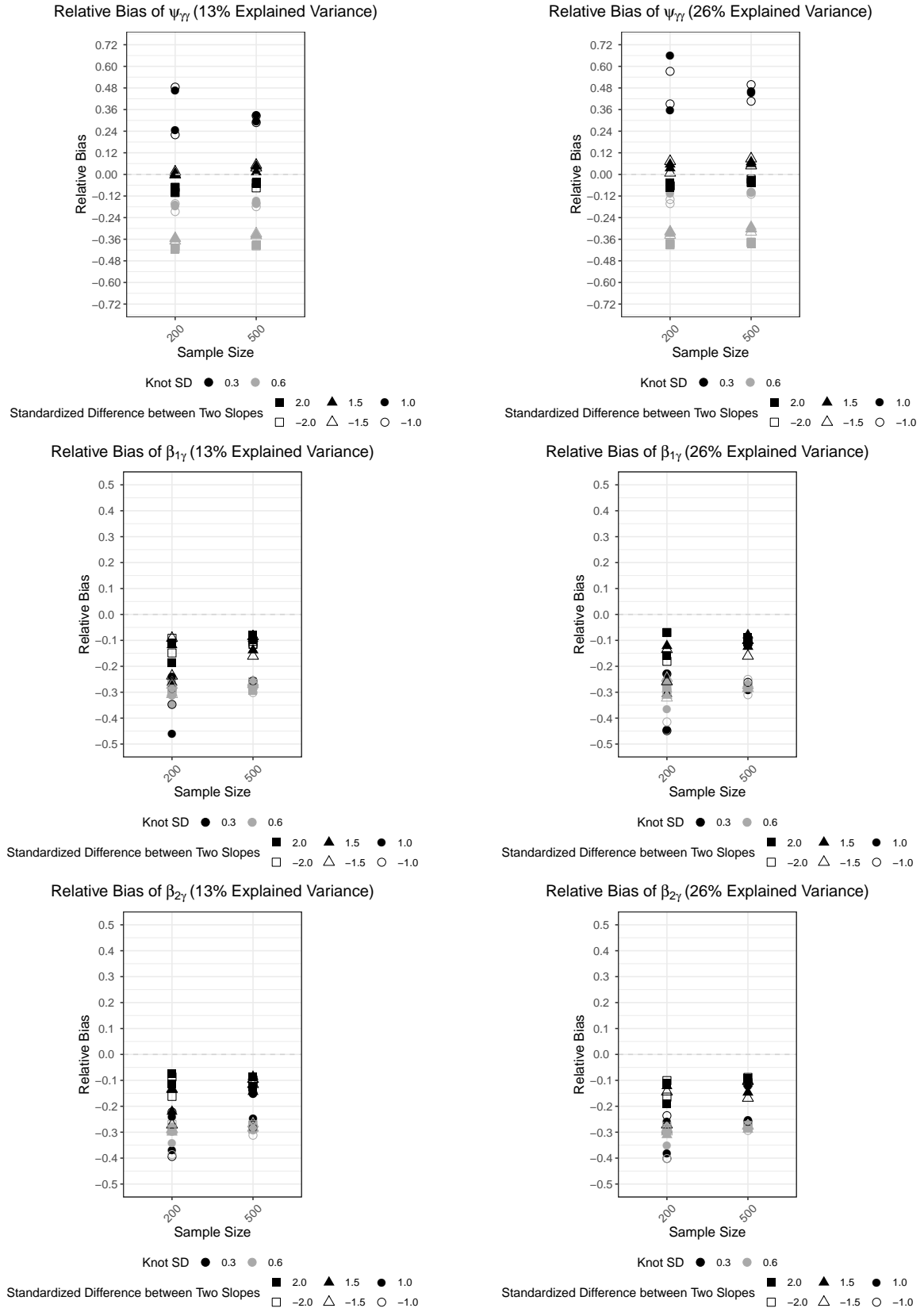
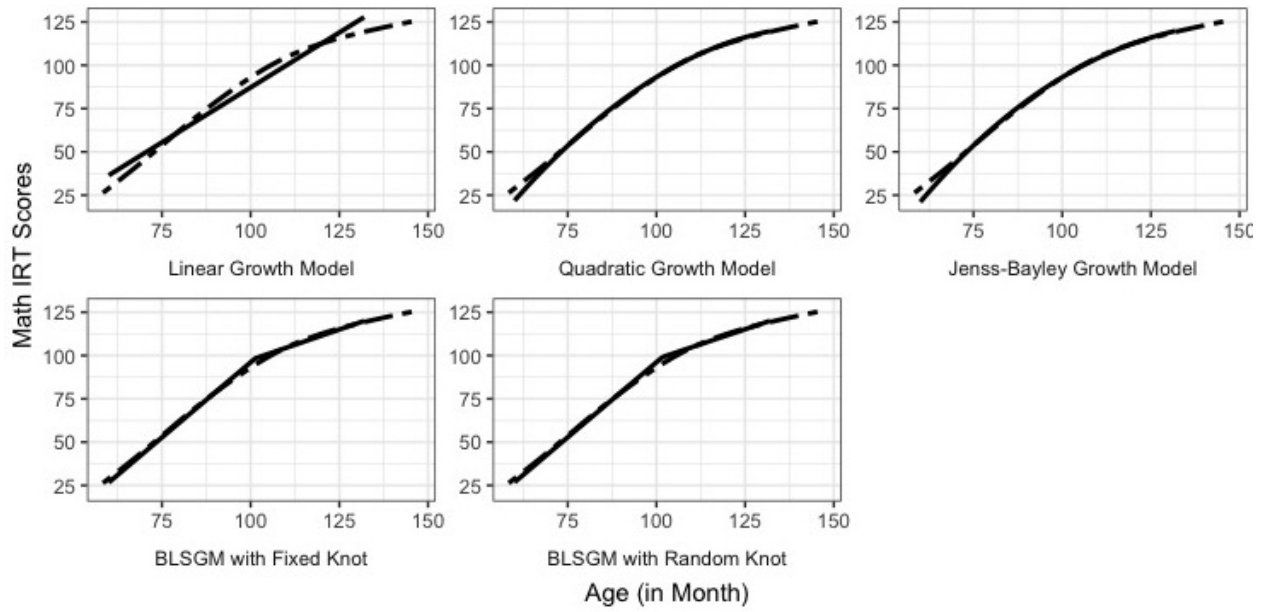


Figure 2: Relative Biases of Path Coefficients and Residuals of Knot under Conditions with 10 Repeated Measures & Midway Knot



Trajectory Type: — Model Implied Math IRT Scores - - Smooth Line of Observed Math IRT Scores

Figure 3: Model Implied Trajectory and Smooth Line of Observed mathematics IRT Scores

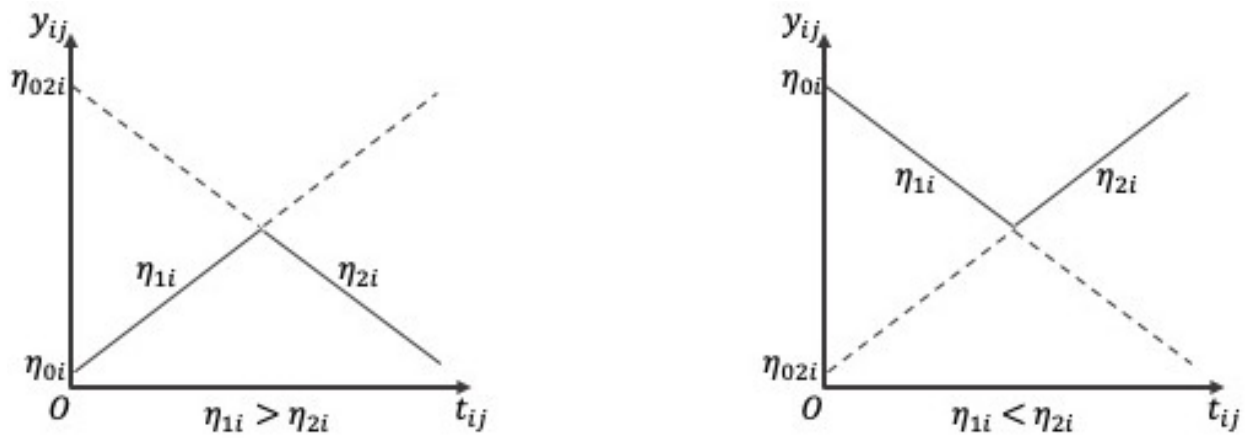


Figure A.1: The Two Forms of the Bilinear Spline (Linear-Linear Piecewise)